

DETERMINATION OF ALPINE TREELINE ECOTONE AND ITS  
SPATIO-TEMPORAL ANALYSIS USING LANDSAT TM IMAGES

A THESIS SUBMITTED TO  
THE GRADUATE SCHOOL OF NATURAL AND APPLIED SCIENCES  
OF  
MIDDLE EAST TECHNICAL UNIVERSITY

BY

GELİNCİK DENİZ BİLGİN

IN PARTIAL FULFILLMENT OF THE REQUIREMENTS  
FOR  
THE DEGREE OF MASTER OF SCIENCE  
IN  
GEODETIC AND GEOGRAPHIC INFORMATION TECHNOLOGIES

SEPTEMBER 2021



Approval of the thesis:

**DETERMINATION OF ALPINE TREELINE ECOTONE AND ITS  
SPATIO-TEMPORAL ANALYSIS USING LANDSAT TM IMAGES**

Submitted by **GELİNCİK DENİZ BİLGİN** in partial fulfillment of the requirements for the degree of **Master of Science in Geodetic and Geographic Information Technologies, Middle East Technical University** by,

Prof. Dr. Halil Kalıpçılar  
Dean, Graduate School of **Natural and Applied Sciences** \_\_\_\_\_

Prof. Dr. Zuhâl Akyürek  
Chairperson of the Department, **Geodetic and Geographic Information Technologies** \_\_\_\_\_

Assoc. Prof. Dr. Uğur Murat Leloğlu  
Supervisor, **Geodetic and Geographic Information Technologies, METU** \_\_\_\_\_

Dr. Uğur Zeydanlı  
Co-Supervisor, **City and Regional Planning, METU** \_\_\_\_\_

**Examining Committee Members:**

Prof. Dr. Zeki Kaya  
Biology, METU \_\_\_\_\_

Assoc. Prof. Dr. Uğur Murat Leloğlu  
Geodetic and Geographic Information Technologies, METU \_\_\_\_\_

Prof. Dr. Zuhâl Akyürek  
Civil Engineering, METU \_\_\_\_\_

Prof. Dr. Çağatay Tavşanoğlu  
Biology, Hacettepe University \_\_\_\_\_

Dr. Semih Kuter  
Forest Engineering, Çankırı Karatekin University \_\_\_\_\_

Date: 10.09.2021

**I hereby declare that all information in this document has been obtained and presented in accordance with academic rules and ethical conduct. I also declare that, as required by these rules and conduct, I have fully cited and referenced all material and results that are not original to this work.**

Name, Last name : Gelincik Deniz Bilgin

Signature :

## **ABSTRACT**

### **DETERMINATION OF ALPINE TREELINE ECOTONE AND ITS SPATIO-TEMPORAL ANALYSIS USING LANDSAT TM IMAGES**

Bilgin, Gelincik Deniz

Master of Science, Geodetic and Geographic Information Technologies

Supervisor: Assoc. Prof. Dr. Uğur Murat Leloğlu

Co-Supervisor: Dr. Uğur Zeydanlı

September 2021, 71 pages

Alpine treeline ecotone (ATE) is the transition zones between forests and alpine grasslands. Because of its ecological importance due to its unique biodiversity, understanding the characteristics of the transition zone is essential. Recent climate change research has shown that the ATE tends to shift upwards. Understanding this upward shift enables the development of climate change indicators for mountain ecosystems and provides insight into efforts towards improving adaptation and mitigation measures.

This thesis aims to develop and apply a methodology for objectively defining and delineating a tree line that is also ecologically meaningful. Another aim is to reveal the shift in ATE for a study area in which this altitudinal shift is expected to have been substantial in the last decades. Within this context, the factors that determine the spatial configuration of the ATE have been investigated through the use of remotely sensed resources. The study area is in the Western Taurus Mountains, located in the Mediterranean region of Turkey.

An algorithm with four steps has been developed to delineate treeline for any given time during the study period, using Landsat images of the relevant years. For each

step, the methodology was chosen with the aim of minimising the need for human interpretation as much as possible and for developing a reproducible method. These steps include obtaining cloud-free seasonal composites from Landsat images, determining tree percentages over the area through spectro-temporal unmixing, and characterising the transition of ATE through fitting a sigmoid response to tree percentages along uphill transects, and modelling of the ATE transition using Random Forest Regression.

Applying this algorithm has revealed that topographical variables combined with information on the percentage of canopy cover can be used effectively while modelling treeline ecotones. Outcomes of the model indicate a downward shift of the treeline on west face of the Dedegöl Mountain for some slopes since 1984, against theoretical expectations or contrary to observations of increases elsewhere in the world. However, on eastern slopes, the shift is indicated to be upwards.

This study can provide input for estimating future shifts in ATE and for further development of models for various climates and latitudes. Also, the algorithm can easily be adapted to other satellite data, thus enabling higher resolution outcomes.

Keywords: Alpine Treeline Ecotone, Treeline, Landsat, Treeline Dynamics, Spatio-temporal Analysis

## ÖZ

### **ALPİN AĞAÇ SINIRI EKOTONUNUN LANDSAT TM GÖRÜNTÜLERİ KULLANILARAK BELİRLENMESİ VE MEKANSAL-ZAMANSAL ANALİZİ**

Bilgin, Gelincik Deniz  
Yüksek Lisans, Jeodezi ve Coğrafi Bilgi Teknolojileri  
Tez Yöneticisi: Doç. Dr. Uğur Murat Leloğlu  
Ortak Tez Yöneticisi: Dr. Uğur Zeydanlı

Eylül 2021, 71 sayfa

Ormanlar ve alpin otsu vejetasyonlar arasındaki geçiş zonu Alpin Ağaç Sınırı Ekotonu (AAE) olarak adlandırılmaktadır. Kendine özgü bir biyoçeşitliğe sahip olmaları nedeniyle ekolojik önem taşıyan bu geçiş zonlarının özelliklerini anlamak giderek daha fazla önem kazanmaktadır. Son zamanlardaki iklim değişikliği araştırmaları, AAE'nin yukarı doğru kayma eğiliminde olduğunu göstermektedir. Bu değişimin haritalanması, iklim değişikliğinin dağ ekosistemlerindeki etkisini ortaya koyan göstergelerin oluşturulmasına katkıda bulunacak ve bu değişim için alınacak önlemlerin belirlenmesine, uyum çalışmalarının planlanmasına yardımcı olacaktır.

Bu tez çalışması, ağaç sınırının ekolojik olarak anlamlı bir şekilde çizilmesini sağlayacak bir yöntem geliştirmeyi ve uygulamayı hedeflemektedir. Bu kapsamda, AAE'nin mekansal özelliklerini belirleyen etmenler uzaktan algılama verileri kullanılarak incelenmiştir. Bu çalışma ayrıca, AAE'nin zaman içindeki kaymasının mekânsal olarak ortaya çıkartılmasını da amaçlamaktadır. Çalışma alanı, Türkiye'nin Akdeniz Bölgesi'nde bulunan Batı Toroslar'dan seçilmiştir.

Ağaç sınırının herhangi bir zaman için ortaya koyulmasını, ilgili yıllara ait Landsat görüntüleri kullanılarak sağlayan dört aşamalı bir algoritma geliştirilmiştir.

Tekrarlanabilir olması amacı ile her aşama için insan değerlendirmesini en aza indirecek yöntemler seçilmiştir. Bu aşamalar; Landsat görüntülerinden bulutsuz mevsim bloklarının elde edilmesi, ayrıştırma yöntemi ile alan için ağaç yüzdesi katmanının oluşturulması, kesitler üzerine sigmoid eğrilerinin yerleştirilmesi yoluyla AAE'nin geçişinin karakterize edilmesi ve "Random Forest" regresyonu kullanılarak AAE'nin modellenmesinden oluşmaktadır.

Tez çalışması kapsamında geliştirilen yöntemin uygulanması, topoğrafik değişkenlerin ağaç kapallığı bilgisi ile birleştirilerek ağaç sınırı ekotonlarının modellenmesinde etkili olarak kullanılabileceğini ortaya çıkarmıştır. Modelin çıktıları, teorik beklentilerin ve dünyadaki bir çok gözlemin aksine, Dedegöl Dağları'nın batı yüzünde 1984-2018 yılları arasında ağaç sınırında oluşan kaymanın bazı yamaçlarda aşağı yönlü olduğunu göstermektedir. Bununla birlikte model, doğu yamaçlarında bu değişimin yukarı yönlü olduğuna işaret etmektedir.

Bu yöntem, AAE'nin gelecekteki kaymasının tahmin edilmesi ve farklı iklimler ve enlemler kullanılarak yapılacak modellerin oluşturulması amacıyla yapılacak çalışmalara girdi sağlayabilecektir. Ayrıca, geliştirilen algoritma kolaylıkla başka uydulardan elde edilecek görüntüleri kullanacak şekilde uyarlanabilir olması sayesinde daha yüksek çözünürlüklü çıktıları olanaklı kılmaktadır.

Anahtar Kelimeler: Alpin Ağaç Sınırı Ekotonu, Ağaç Sınırı, Landsat, Ağaç Sınırı Dinamikleri, Mekansal-zamansal Analiz



Dedicated to mountains

## ACKNOWLEDGMENTS

I wish to express my deepest gratitude to my supervisor, Assoc. Prof. Dr. Uğur Murat Leloğlu for his knowledge, patience and helpfulness and also for always making time to help. I would also like to thank my co-supervisor Dr. Uğur Zeydanlı for providing support and guidance whenever I needed it.

I have understood once more that I am a very lucky person to have parents like mine. I am grateful to my parents, Ayşe S. Turak and C. Can Bilgin, not only for being supportive and loving parents but also for the guidance and knowledge they have provided me with through the realization of this thesis.

I want to thank Prof. Dr. Zuhale Akyürek for the GIS course she teaches and the internship with her, which made me realize that I could use my background as a civil engineer in other areas. I am grateful for these opportunities that helped me find a reason to finish my undergraduate studies even though I was not too fond of the department. I am also grateful to the other jury members Prof. Dr. Zeki Kaya, Prof. Dr. Çağatay Tavşanoğlu, and Assist. Prof. Dr. Semih Kuter, for their constructive and insightful comments, to improve this thesis study.

I want to express my gratitude to my colleagues in DKM, from whom I have learned a lot. I especially want to thank Dr. Semiha Demirbaş Çağlayan and Dr. Tuba Bucak for their patience, guidance and friendship.

I would like to thank Erkan Aşık, Yücel Torun, Güven Kazım Altunkaya, Seda Dolaner and Sıla Akman for their most valuable friendship. I would also like to express my appreciation of İpek Gül Karasu, my oldest friend, whom I see as a sister.

I want to thank my friends Melisa Çelik, Elif Bekoğlu for their solidarity when I needed it the most. A special thanks to Seçil Güler for always understanding and encouraging me. I also want to thank Çiğdem Ekiz for being the best neighbour.

Last but not least, I would like to thank my sister Yasemin Bilgin and my partner Mert Bilgiç. You are the people that add meaning to my life.

## TABLE OF CONTENTS

ABSTRACT .....	v
ÖZ .....	vii
ACKNOWLEDGMENTS .....	x
TABLE OF CONTENTS .....	xii
LIST OF TABLES .....	xv
LIST OF FIGURES .....	xvi
LIST OF ABBREVIATIONS .....	xix
CHAPTERS	
1 INTRODUCTION .....	1
1.1 Problem Definition .....	1
1.2 Purpose and Scope .....	3
1.3 Contribution of Thesis to Literature .....	3
1.4 Organization of the Thesis .....	4
2 LITERATURE REVIEW .....	5
2.1 Alpine Treeline Ecotone .....	5
2.1.1 Definitions .....	5
2.1.2 Status in the Past Decades .....	9
2.2 Factors that Determine the ATE .....	10
2.3 Remote Sensing of the ATE .....	12
2.3.1 Delineation of the ATE .....	13
2.3.2 Change detection .....	13

2.4	Studies regarding the methods used in this thesis .....	14
2.4.1	Cloud removal.....	14
2.4.2	Unmixing using multi-temporal indices .....	15
2.4.3	Sigmoid curve fitting to describe ecotone transition characteristics.	15
2.4.4	Random forest regression .....	16
3	STUDY AREA AND DATA.....	17
3.1	Study Area.....	17
3.2	Satellite Data and Problems .....	19
3.2.1	Landsat TM Data .....	19
3.3	Ancillary Data .....	23
4	ALGORITHM FOR DELINEATION OF THE ATE .....	25
4.1	Summary of the Algorithm .....	25
4.2	Cloud removal and calculation of indices .....	26
4.2.1	Cloud removal.....	26
4.2.2	Calculation of indices .....	27
4.3	Transects for examination of the treeline transition.....	28
4.4	Unmixing using multi-temporal indices.....	30
4.4.1	Endmember selection.....	30
4.4.2	Unmixing process .....	31
4.4.3	Calculation of tree percentage .....	31
4.5	Fitting of sigmoid waves to the transition of ATE.....	32
4.6	Random Forest Regression and Model .....	34
5	RESULTS AND DISCUSSION .....	39
5.1	Outputs of the Algorithm .....	39

5.1.1	Cloud removal and calculation of indices .....	39
5.1.2	Transects .....	42
5.1.3	Unmixing .....	44
5.1.4	Fitting of sigmoid waves .....	52
5.1.5	Random forest regression and model .....	54
5.2	Change of treeline position from 1984 to 2018, Dedegöl Mountain .....	58
5.3	Discussion .....	61
6	CONCLUSIONS .....	63
	REFERENCES .....	65

## LIST OF TABLES

### TABLES

Table 3.1 Available cloud-free images of the study area.....	21
Table 3.2 Topographic variables and calculation scales.....	24
Table 4.1 First ten rows of the matrix for the model input, for Dedegöl Mountain. .....	35

## LIST OF FIGURES

### FIGURES

Figure 2.1. A typical treeline ecotone in the Taurus Mountains range Photo: UML 6	
Figure 2.2. Gradual transition of ATE.....	7
Figure 2.3. Sharp transition of ATE .....	7
Figure 2.4. Change of form through the ATE: Tree to shrub.....	8
Figure 2.5. Change of form through the ATE: Tree to krummholz .....	8
Figure 3.1. Dedegöl Mountain’s location in Turkey .....	17
Figure 3.2. Dedegöl Mountain study area .....	18
Figure 3.3. Cloudy Landsat image of 25 <sup>th</sup> of April, 2018, Dedegöl Mountain .....	20
Figure 3.4. Landsat image of 3 <sup>rd</sup> of September, 2018, Dedegöl Mountain .....	22
Figure 3.5. Digital elevation model of the Dedegöl Mountain study area .....	23
Figure 3.6. Derived topographical layers .....	24
Figure 4.1. Summary of the flow of the algorithm.....	25
Figure 4.2. Contours on DEM, Dedegöl Mountain .....	29
Figure 4.3. 1800 m contour and its smoothing, Dedegöl Mountain.....	29
Figure 4.4. From left to right: original transect, part after the maximum elevation was eliminated, the part before the minimum elevation was eliminated.....	32
Figure 4.5. An example of before and after the elimination of elevation drops. Filled grey parts were eliminated.....	33
Figure 4.6. An example of fitted sigmoid wave and its normalization .....	34
Figure 4.7. The output of the random forest regression, 2018, Dedegöl Mountains .....	37
Figure 5.1. Cloudless April – June image for 2018, Dedegöl mountain .....	40
Figure 5.2. Cloudless July – August image for 2018, Dedegöl mountain.....	40
Figure 5.3. Cloudless September – October image for 2018, Dedegöl mountain...	40
Figure 5.4. Cloudless November – March image for 2018, Dedegöl mountain .....	40
Figure 5.5. Seasonal indices calculated for 2018, Dedegöl Mountain .....	41
Figure 5.6. Correlation of indices.....	42



Figure 5.7. DEM, 1800 m contour and transects for the Dedegöl Mountain.....	43
Figure 5.8. NDVI variation through seasons for endmembers .....	45
Figure 5.9. EVI2 variation through seasons for endmembers .....	45
Figure 5.10. NDWI variation through seasons for endmembers .....	46
Figure 5.11. NDSI variation through seasons for endmembers.....	46
Figure 5.12. Insert figure caption here .....	47
Figure 5.13. Results of unmixing for the endmembers, Dedegöl mountain .....	48
Figure 5.14. Results of unmixing for the endmembers, and the RSME .....	49
Figure 5.15. Results of unmixing extracted for a transect as an example.....	49
Figure 5.16. Percentage of trees, 2018, Dedegöl Mountain.....	50
Figure 5.17. Comparison of tree abundance changes from 1984 to 2018, generated using spectral bands and normalized difference indices .....	51
Figure 5.18. Histogram for correlation of sigmoid fits to the tree abundances of input sample points .....	52
Figure 5.19. Examples of successfully fitted transects (correlation > 90%) .....	53
Figure 5.20. Examples of poorly fitted transects (correlation < 90%).....	53
Figure 5.21. Error versus the number of variables for the regression.....	54
Figure 5.22. Predictor variable importance plot .....	55
Figure 5.23. Accuracies of training and test data.....	55
Figure 5.24. An example from model output, calculated using 2018 images, Dedegöl Mountain .....	56
Figure 5.25. An example from model output, calculated using 2018 images, Dedegöl Mountain .....	56
Figure 5.26. An example from model output, calculated using 2018 images, Dedegöl Mountain .....	57
Figure 5.27. An example from model output, calculated using 2018 images, Dedegöl Mountain .....	57
Figure 5.28. Comparison of 1984 and 2018 Treelines, western slopes of Dedegöl Mountain .....	59

Figure 5.29. Comparison of 1984 and 2018 treelines, north slopes of Dedegöl Mountain.....59

Figure 5.30. Comparison of 1984 and 2018 upper limit of ecotones, east slopes of Dedegöl Mountain. .... 60

Figure 5.31. Barplot showing the change in treeline altitude..... 61

## LIST OF ABBREVIATIONS

### ABBREVIATIONS

ATE: Alpine treeline ecotone

DEM: Digital elevation model

EVI: Enhanced vegetation index

FCLS: Fully constrained least squares

NDSI: Normalized difference soil index

NDVI: Normalized difference vegetation index

NDWI: Normalized difference water index

NDX: Normalized difference indices

NNLS: non-negative least squares

NIR: Near-infrared

RF: Random forest

RMSE: Root mean square error

RS: Remote sensing

RS data: Remotely sensed data

SCA: sequential coordinate-wise algorithm

SWIR: Short-wave infrared

TRI: Topographic roughness index

TPI: Topographic position index

TWI: Topographic wetness index



# CHAPTER 1

## INTRODUCTION

### 1.1 Problem Definition

In nature, distributions of organisms are restricted by physical boundaries such as soil, water, climatic properties, which characterize the ecosystems. Ecotones are transition zones between different types of ecosystems. Transitions from a forest to a field or from a lake to grassland are abrupt and easily recognized with the changing environmental conditions. In contrast, the transition between steppe and humid grasslands due to the changing slope resulting in increased soil moisture is not easily identified. Moreover, the change in environmental conditions may be gradual, resulting in a gradual transition, and thus, a wider ecotone.

These areas are often inhabited by species common to both neighbouring communities and also with species that are specific to the transition area. Ecotones are important in terms of ecology since biodiversity is increased and genetic diversity is high. Also, ecotones play a role in landscape stability, as they act as a semi-permeable membrane between the two systems (Farina, 2008).

Alpine treeline ecotone (ATE), or shortly treeline, is the transition zone between forest and treeless grasslands in mountainous environments (Dinca et al., 2017). This transition can be abrupt or in a diffused manner where the density and tree heights decrease gradually, or the form of the trees can change into shrub form or irregular forms with the altitude.

With the changing climate, ecotones are expected to respond to this change by shifting spatially. ATE is a suitable ecotone to monitor this response and can act as an indicator of climate change. In addition to the aforementioned importance of ecotones, ATE can serve as a refuge for species that are affected by direct and

indirect effects of climatic changes and other disturbances, such as trees surviving beetle outbreaks (Maher et al., 2021). The spatial configuration of the ATE depends on many factors such as topographical, edaphic, climatic, and anthropogenic variables. And as these variables change, the ATE also changes (Körner, 2012).

For example, as the climate changes, snow cover, moisture regime, and nutrient conditions change. A large number of studies on ATE have shown its trend to shift upwards, especially if strong winter warming is present (Harsch et al., 2009). Given the ecological importance of the ATE, investigation of change in its pattern would be essential to produce data for adaptation and mitigation measures.

Remote sensing methods are being used for monitoring ecology, biodiversity, and conservation metrics with an increasing frequency, due to their convenience. Using remote sensing to monitor larger extents or areas where the accessibility is low reduces the cost and time spent on the study (Kerr and Ostrovsky, 2003). Moreover, using remote sensing, more frequent sampling is possible with less effort compared to in situ studies. Thus, remote sensing is convenient for vegetation monitoring of mountainous areas.

The use of automated processes for data generation from remotely sensed images widens the scope of outputs that can be obtained. Compared to manual generation of data, for example, visual interpretation of images, automation saves time and improves precision by eliminating the perspective differences of different experts. In other words, it provides standardization for the generation of data. By using an algorithm that combines the automated processes, the solution can be applied to similar areas.

For monitoring the ATE and its change over time, a standardized and objective method proves to be essential. The portrayal of the nature of the transition is needed for understanding the importance of factors that determine the spatial configuration of the treeline.

Landsat data goes back furthest of all remotely sensed multi-spectral imagery data, making it appropriate for monitoring long-term trends. Also, its availability for

public use makes it the most appropriate source of data for many studies (Kennedy et al., 2014). As treelines change in a slow manner, considering the largest possible window of time is essential. Landsat 5 and its predecessors have provided data since 1984, with seven spectral bands and a spatial resolution of 30 m (NASA, 2021).

## **1.2 Purpose and Scope**

Firstly, this thesis aims to develop an objective and easily repeatable algorithm to delineate the ATE and characterize the transition using Landsat TM data.

Secondly, this thesis aims to analyse the contribution of different variables to the spatial configuration ATE.

The third aim of this thesis is to investigate the change of ATE for the study area, using multi-temporal Landsat data via the algorithm developed.

## **1.3 Contribution of Thesis to Literature**

This thesis aims to develop a new algorithm to delineate the treeline;

- objectively,
- by using an easily repeatable method,
- by characterizing the form of transition,
- by using easily accessible data and software.

With the data that is provided, further ecological investigations can be done. If the reason for the change can be identified, such as the change in the climate or human use, this information can be used for developing a conservation plan if the ecosystem is under threat.

Also, this study is the first research on ATE change and the second study on the delineation of the ATE, conducted in Turkey.

## **1.4 Organization of the Thesis**

In the second chapter, detailed background information is given, and the relevant studies present in the literature are described.

In the third chapter, information about the study area and also all of the data used in this thesis is given. Acquisition and the pre-processing stages of the data are also explained in this chapter.

In the fourth chapter, the development of the algorithm to delineate the ATE is presented. Furthermore, the accuracy assessment is given.

In the fifth chapter, results are given and discussed.

In the sixth and the last chapter, the conclusions of this thesis study are presented.



## CHAPTER 2

### LITERATURE REVIEW

#### 2.1 Alpine Treeline Ecotone

##### 2.1.1 Definitions

Alpine treeline ecotone or treelines are defined slightly differently in various sources. Moreover, various names are used for similar concepts. For example, forest line can be defined as the transition zones between the forests and treeless grasslands (Dinca et al., 2017). On the other hand, the alpine treeline can be defined as the upper limit of elevation where individual trees beyond it are smaller than two meters (Kullman, 1979). Another naming is treeline forests, and it is defined as a physiological threshold where the tree form becomes not viable (Zhang et al., 2009).

Christian Körner (2012) states that the “tree” from the Alpine treeline is the life form, not species. As the conditions get harsher, the upright tree form gets less suitable for woody vegetation. So the trees stay in the sapling or shrub form, or they take irregular forms due to continuous exposure to freezing winds, which is called *krummholz*. The Ecotone that Körner defines in the book is the transition zone between the tree form and the upper alpine vegetation forms, i.e., shrubs and grassland. The tree species can still occur in different forms above this ecotone. In this thesis, the definition of treeline is based on Körner’s.

The transition can be sharp and can even form a line when the change in environment is more significant. For example, in mild slopes, it can be diffused so that the canopy opening increases and tree size decreases gradually, resulting in the ecotone being wide. Examples of forms of transition zones are given in the below photo and sketches (Figure 2.1, Figure 2.2, Figure 2.3, Figure 2.4, and Figure 2.5).



Figure 2.1. A typical treeline ecotone in the Taurus Mountains range Photo: UML

Usually, instead of one line, two or three lines are used for defining the ATE; lower and upper treeline, and on occasion, a mid-line.

In most studies, timberline refers to a boundary where crown closure and tree height decreases lower than some point. Several studies specify these limits using different values, which depend on the species of the trees at the ecotone (Holtmeier, 2009).

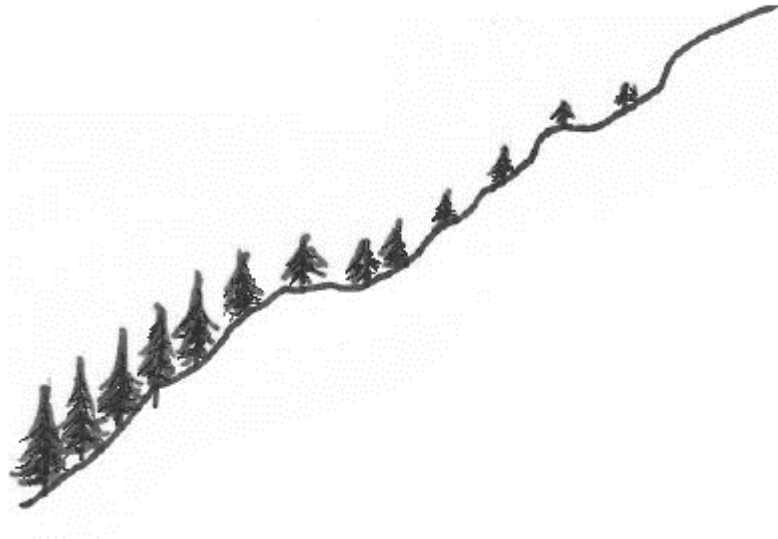


Figure 2.2. Gradual transition of ATE

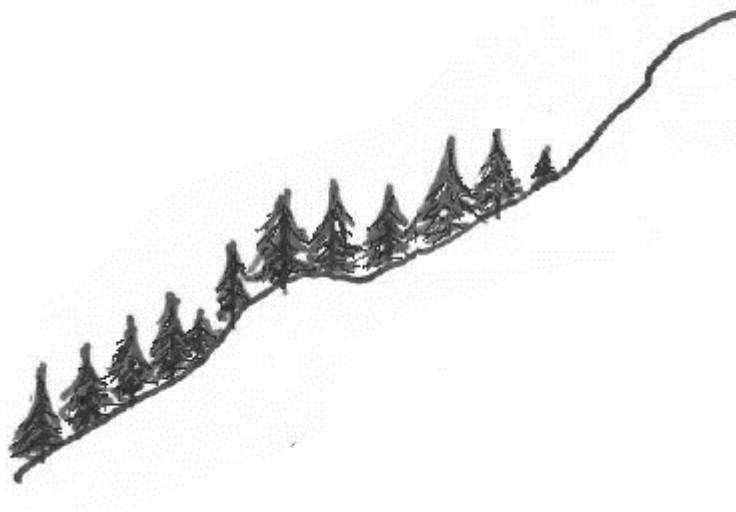


Figure 2.3. Sharp transition of ATE

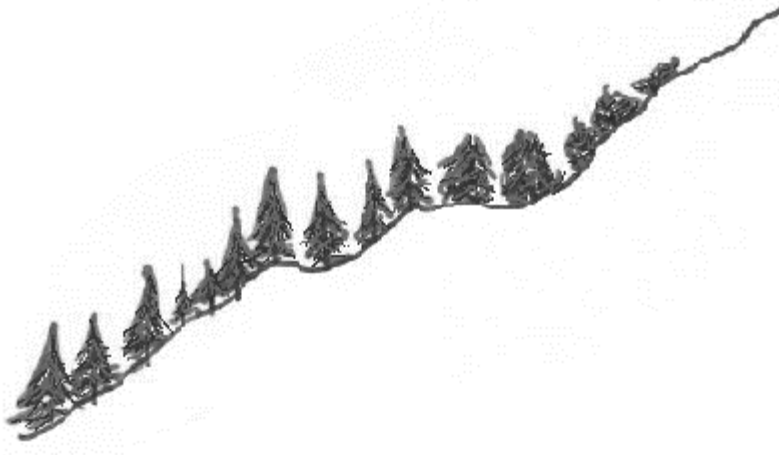


Figure 2.4. Change of form through the ATE: Tree to shrub

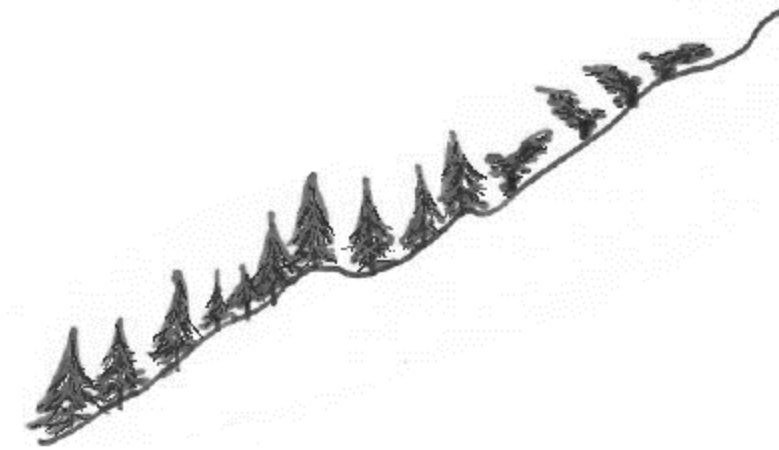


Figure 2.5. Change of form through the ATE: Tree to krummholz

### **2.1.2 Status in the Past Decades**

A study conducted by (Harsch et al., 2009) that examines globally distributed 166 sites that the treeline dynamics have been recorded for over a century reveals that 52% of them are advancing, and only 1% is in recession. They also state that treelines with a smooth transition or where the winter temperatures increased substantially are more likely to shift upwards. Furthermore, where no advancement is recorded, the area is more likely to have other constraints than climate that limits tree growth.

Another study with hundred years of observation at the European Alps shows a 115 m increase followed by an accelerated increase of 10 m at eight years. Showing that the changes in Alpine treeline ecotones have accelerated in the past decades as climate change became more prominent. Observed for a period of 25 years using Landsat images, the ATE in Glacier National Park, USA, has become greener over this period. This increase in NDVI suggests that an upwards shift is present at the ATE (Potter, 2016). Furthermore, some studies point to an increase in tree abundance near the treeline, although it is not increasing or decreasing in the lower parts of the forest (Chen et al., 2015).

In contrast, another study reveals that in Sierra Nevada Mountains, there is no evidence of an increase in canopy leaf cover in subalpine forest stands. Furthermore, significant loss of canopy cover is observed for Sierra whitebark pine (Potter and Dolanc, 2016). Likewise, there are more sites where the treeline is stationary (Zhang et al., 2009) or decreasing (Kullman, 2005).

As the temperature is a limiting factor for growth at ATE's, temperature increase means higher altitudes can become suitable for trees, making climate change the primary driver of changes of treelines (Grace et al., 2002). Another limiting factor that inhibits tree growth is grazing. With the decreasing human population in rural areas, grazing pressure on forests is decreasing in some regions. The absence of grazing pressure may be causing the ATE to change (Gehrig- Fasel et al., 2007).

As the spatial configuration of Alpine treelines changes, the biodiversity of these ecotones is impacted. In response, the effect of animals, especially the herbivorous

ones, have an impact on the ATE, in most cases as pressure upon it (Wielgolaski et al., 2017).

## **2.2 Factors that Determine the ATE**

Although the altitude is the most obvious one, the spatial configuration of treeline ecotones in mountainous regions depends on various factors. Moreover, these dependencies change as the scale of the area of interest changes. For example, when a small area like one hillside of a mountain is observed, differences in precipitation amounts become irrelevant for shaping the ATE, as it would be similar all over the hillside. However, if the area of interest is a range of mountains, precipitation amounts would differ at the south and north sides of the mountains (Malanson et al., 2013; Weiss et al., 2015).

Species composition at the subalpine forest plays a vital role in shaping the treeline position since the ability to adapt to the harsh conditions of mountainous environments of each tree species varies (Weiss et al., 2015).

As mentioned earlier, ATE's are highly influenced by climatic drivers. As the altitude increases, temperatures decrease, limiting the photosynthesis process and making it less suitable for a tree to grow (Grace et al., 2002). Solar radiation also has an indirect relation to the photosynthesis process. Plants close their stomata to prevent moisture loss as a response to high radiation, but at the same time, this reduces the CO<sub>2</sub> entrance, limiting photosynthesis (Cairns and Malanson, 1998). Soil temperature plays a critical role in tree growth, even more important than air temperature (Körner and Hoch, 2006). Precipitation, especially in spring, plays a vital role in tree growth at the treeline (Sigdel et al., 2018). Furthermore, snow accumulation, spring snow duration, and avalanche paths have an influence over the position of the ATE (Elliott and Petrucci, 2018; Walsh et al., 1994)

Topographic drivers have an important role in the alignment of treelines. Several studies point out that slope and aspect are the main drivers of alpine treelines (Bader and Ruijten, 2008; Dalen and Hofgaard, 2005; Elliott and Kipfmüller, 2010). Slope

and aspect determine the amount of solar radiation and creates microclimatic differences, resulting in treelines at different altitudes. These differences gain more importance for finer scales (Elliott and Cowell, 2015). Moreover, aspect and slope influence the composition of plant communities over the ecotones, making them significant drivers (Dearborn and Danby, 2017). In addition to slope and aspect, SPI (Snow potential index) and wetness index, which are derived using topography, can be used as proxies for drivers that control the configuration of ATE (Zong et al., 2014).

The location and configuration of the site are influential on the treelines. The aspect of the slopes has different effects on the treelines at different scales. For example, being located on the north side of the mountain and a north side of a small valley on the south-east side of the mountain has different effects on the treeline position. Thus, the slope aspect, which can be indicated by the Northness and Eastness parameters, is a valuable parameter that shapes the treeline (Bader and Ruijten, 2008). Also, moving from the equator to the poles, the altitude of treelines decreases, making latitude an important variable. Furthermore, as continentality increases, the treelines move to higher altitudes (Caccianiga et al., 2008; Körner, 2012).

Geomorphology and geology are other factors that affect the treeline configuration, and they can be either limiting or promoting advance. Large boulders, flat areas below steep slopes or rock walls can provide refuge from the harsh conditions of the mountain, such as strong winds, and promote sapling growth (Resler, 2006). Soil depth is inversely correlated with moisture stress, and as the soil depth increases, trees become more resistant to moisture stress (Cairns and Malanson, 1998). Soil organic matter decreases with the increasing elevation, limiting the tree growth (Müller et al., 2017). However, higher fertility of soil does not always mean a higher treeline since other alpine vegetation may be more competitive than the woody species (Malanson and Butler, 1994). Lithology and geologic structure can limit the ATE from reaching the climatic optimum (Butler et al., 2007). For example, slopes with scree may not be able to support seedling growth as the movement and lack of

organic material results in an unsuitable condition. Likewise, rock walls can act as a barrier and an unfavourable medium for seedling growth.

Lastly, anthropogenic factors have effects on the ATE and sometimes can drastically inhibit its advancement to the climatic optimum. While grazing acts as a limiting factor, abandonment of former grazing areas can lead to an upwards shift in the ATE (Gehrig- Fasel et al., 2007). Although wood production and agricultural practices are usually not feasible at the altitude of treelines, combined with other limiting factors, those practices can have adverse effects on the ATE.

### **2.3 Remote Sensing of the ATE**

Mountain ecosystems, with their rough terrain, have problematic and expensive accessibility, making them hard to monitor using in-situ studies. Moreover, for studies on a scale that focuses on whole mountains, the need for extensive examination arises. Remote sensing offers an alternative to field study, enabling remote and large areas to be examined cheaper and easier.

For studies of treelines, which usually require surveillance of large areas, remote sensing is an invaluable tool. Furthermore, the ATE does not have a homogeneous spatial distribution, making it suitable for remote sensing studies (Weiss and Walsh, 2009).

For studies that focus on delineation or change of treelines, remotely sensed data is an important source. Various methods can be used for these research topics, such as vegetation classification or using indices. Also, satellite data and aerial images can be used individually, as well as combined together, which can be from different sources (Fissore et al., 2015).

Earlier treeline dynamics research that used RS mainly focused on mapping the position of the treeline and used low or moderate resolution satellite data. With the arrival of higher resolution satellite sensors, a new focus on the limiting factors that determine the ATE arises (Chhetri and Thai, 2019).



### **2.3.1 Delineation of the ATE**

In the process of determining the spatial position of the ATE using RS data, vegetation classification is the most common approach, where supervised and unsupervised methods are used (Fissore et al., 2015).

For situations where moderate resolution satellite data, such as Landsat, is available, using vegetation indices like NDVI can be preferred rather than hard classification due to its ability to provide a continuous representation of the vegetation cover at the transition zones (Zhang et al., 2009). This restriction of hard classification can also be avoided by using soft classification methods that provide an output of class membership probabilities, alongside the use of higher resolution RS images (Hill et al., 2007).

#### **2.3.1.1 Methods for Landsat Data**

Remotely sensed data provided by Landsat satellites is favoured by many researchers due to the accessibility of years' worth of data. As mentioned earlier, most of the studies that use Landsat data use NDVI to delineate the treeline. More complex models use additional inputs, which are environmental variables.

### **2.3.2 Change detection**

For change detection, most of the studies prefer to examine NDVI difference through the period in question. This method gives an idea of the change, even with coarse resolutions, because a small amount of greening in a sparsely vegetated pixel can influence the NDVI value considerably (Masek, 2001).

A research conducted in southern Italy, which uses Landsat imagery with NDVI differencing, shows that high accuracy results are possible with this method and reveals that forest cover has increased significantly through the period 1984-2010 (Mancino et al., 2014).

Other than NDVI differencing, regression and classification models are used. A study combines NDVI values of 30 years and topographical data to use in time series second-order polynomial regression (Potter and Dolanc, 2016). Another study, which is from Köprülü Kanyon, Turkey, uses aerial photographs, stand maps, and very high-resolution satellite data to perform coarse classification in order to detect the changes in a stand scale (Karahalil et al., 2009).

Linear spectral mixture analysis can also be used for change detection. Abundance change over a period can be used as a measure for the change of treeline (Chen et al., 2015).

## **2.4 Studies regarding the methods used in this thesis**

### **2.4.1 Cloud removal**

With low temporal resolution satellite data, the presence of clouds is a common problem. This can result in long periods without a usable image (Ju and Roy, 2008). Some studies use only the image itself to recover the small cloudy patches geometrically. However, this approach leads to high biases for large clouds. Another approach is to model the cloudy bands with cloud-free bands. An example of this would be using the NIR band of Landsat TM images for haze reduction (Ji, 2008). Nevertheless, this approach would be sufficient for images with thick cloud cover. Furthermore, using data from multiple satellite complementation of the cloudy patches could be performed, which is a costly computation in terms of time and effort. Lastly, cloud removal can be done using multi-temporal images to complement the cloudy patches. (Chen et al., 2017).

Cloud removal using multi-temporal images can be done pixel-based or patch-based. Furthermore, more complex non-linear methods can be used to minimize radiometric inconsistency (Lin et al., 2014).

### **2.4.2 Unmixing using multi-temporal indices**

Since Landsat has a moderate spatial resolution, spectral mixture analysis, in other words unmixing, is a valuable tool to understand the components of each pixel of the image. Unmixing of Landsat images and other moderate resolution satellite data can be effectively used to understand the forest cover fractions and analyse forest areas where canopy cover is open or closed, or have a mixture of vegetation types. Furthermore, it is an invaluable tool for detecting change through time (Senf et al., 2020).

One study shows that unmixing with normalized difference indices can provide more accurate results compared to bands obtained by using principal component analysis with simple mixture models. Although using normalized indices may be problematic due to their nonlinearity, improvement of the results was observed (Rogers and Kearney, 2004). In addition, the effect of shadows on images can be minimized by using normalized difference indices.

### **2.4.3 Sigmoid curve fitting to describe ecotone transition characteristics**

For studies that focus on the ecotone rather than one ecosystem, modelling the transition zone in a precise way is essential. Although some ecotones may be abrupt and can even be defined as a line, defining them using fuzzy classifications would be a more inclusive approach (Fisher et al., 2006). Sigmoid wave fitting is one of the methods used for defining ecotones in such a way. This method provides a robust approach to model ecotones that vary in steepness, patchiness, and width (Hufkens et al., 2008).

At alpine treeline ecotones, tree cover percentages decrease as the altitude increase. A decreasing sigmoid curve fitted to the tree cover percentages represents the transition successfully, especially where it is shaped by climate (Cairns and Waldron, 2003).

#### **2.4.4 Random forest regression**

Random forests (RF) (Breiman, 2001; Ho, 1995) is a powerful statistical machine learning tool that can be used for ecological prediction models. Several studies show that it often outperforms other commonly used methods for this field of study. RF provides a robust approach that considers the predictor importance (Fox et al., 2017).

Random forests can be used for performing regression and classification. RF also provides parameter importance information (Liaw and Wiener, 2002), which is essential for understanding the treeline ecotones dynamics, since determining the shaping factors is a prerequisite for that insight.

For modelling the subalpine forests and the ATE, RF is used for various purposes such as classification, estimation of forest cover, calculation of variable importance, and creating a model using forest cover (Landry et al., 2018; McCaffrey and Hopkinson, 2020; Resler et al., 2014).

## CHAPTER 3

### STUDY AREA AND DATA

#### 3.1 Study Area

The study area used in this thesis is the Dedegöl Mountain.

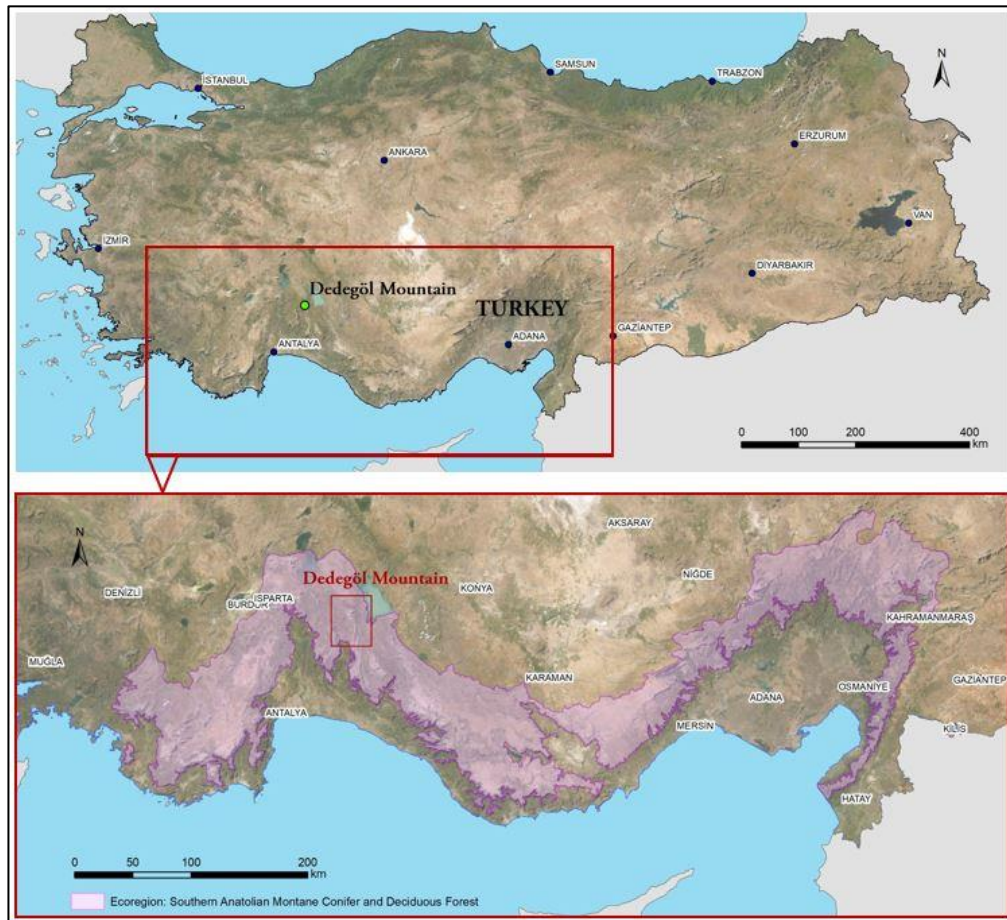


Figure 3.1. Dedegöl Mountain's location in Turkey

Dedegöl Mountain is located at the East of Isparta, near Yenişarbademli, and it is a part of the Western Taurus Mountains. Beyşehir Lake is located at its East. It has a

peak with a 2992 m elevation. The area ranges from N 37 34 to N 37 42 and from E 31 18 to E 31 40.

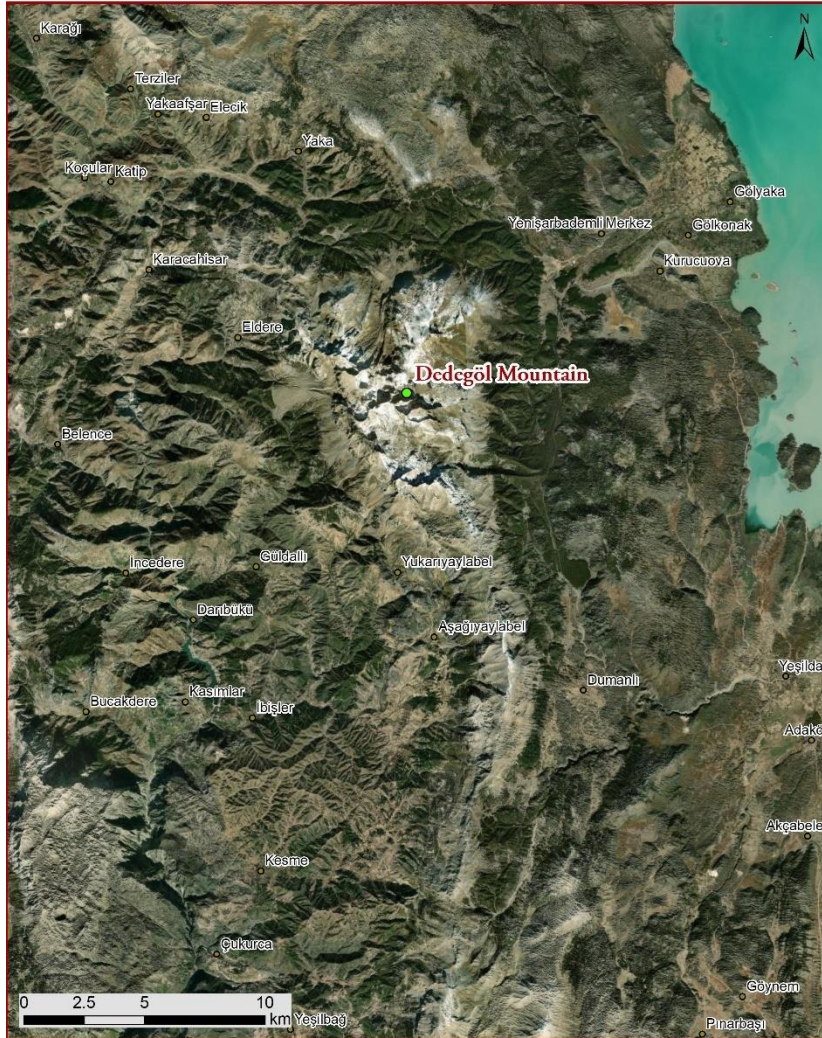


Figure 3.2. Dedegöl Mountain study area

Woody vegetation cover around the mountain consists primarily of coniferous trees and shrubs. Black pine (*Pinus nigra*) and cedar (*Cedrus libani*) are the dominant species at the east side of the mountain, near the treeline, alongside Greek juniper (*Juniperus excelsa*) and fir (*Pinaceae abies*). The north side consists of black pine, kermes oak (*Quercus coccifera*), and occasionally cedar and deciduous oaks. Black pine, Greek juniper, and kermes oak are the dominant species located on the west side of the mountain alongside cedar and deciduous oaks.

## **3.2 Satellite Data and Problems**

This thesis aims to create an algorithm that can be used to determine the past state of the ATE and subsequently to provide a tool for examination of the change of ATE through periods. Consequently, Landsat images were chosen to be used in the algorithm. Although the resolution of 30 m presents itself as a drawback in accurately defining the transition of the ecotone, being easily accessible and dating back to 1985 with 30 m resolution makes Landsat data the most appropriate satellite data for this thesis.

### **3.2.1 Landsat TM Data**

#### **3.2.1.1 Acquisition**

In order to make the data download process easily repeatable, a code was written using Google Earth Engine (GEE). This code was constructed to select the images from the target year and support years where the total cloud cover of the image is smaller than 10%. Then, using GEE's function simple cloud cover, the cloud cover of each pixel in each image was calculated. Finally, the cloud cover raster was added to the images as a band to be downloaded in TIFF format.



### 3.2.1.2 Cloud Problem

As the area of interest is mountainous, obtaining cloud-free images is a problem. When the Landsat TM images of 2018 and 2019 are examined, as presented in Figure 3.3, it can be seen that there are not enough cloud-free images to form meaningful seasonal composites, especially for the spring.



Figure 3.3. Cloudy Landsat image of 25<sup>th</sup> of April, 2018, Dedegöl Mountain



Table 3.1 Available cloud-free images of the study area

	2018	2019
January	19th	-
February	-	-
March	-	-
April	-	-
May	-	14th
June	-	-
July	-	1st
August	15th	-
September	-	19th
October	18th	-
November	3rd	6th
December	21st	8th

A study about the land-cover classification of areas where it is frequently clouded proposes to use images of multiple years, using scores to create one cloudless image. The importance of the pixels decreases as the distance between the target year and the year of the used image increases, whereas they increase as the cloudiness decreases (Man et al., 2018). To overcome the cloud problem, this method was simplified and used in this thesis.

### 3.2.1.3 Shadow Problem

Shadow presence often leads to classification problems or erroneous results in change detection in remote sensing applications. Since the shadows present on an area change depending on the imaging time and season, the remotely sensed images must be modified prior to use. This can be done either by producing shadow-free images or reducing the impacts of the shadow variability of images (Shahtahmassebi et al., 2013).



Figure 3.4. Landsat image of 3<sup>rd</sup> of September, 2018, Dedegöl Mountain

The above Landsat image (Figure 3.4) shows that north-facing slopes are dark, and south-facing faces are bright. This causes similar compositions of vegetation to have different reflectance values depending on the direction they face.

There are many indices developed for vegetation monitoring using multiple spectral wavebands, and they are widely used due to their simplicity and practicality. Most of the widely used ones are normalized difference indices which eliminate the effects of shadows using ratios of various bands.

For sparsely vegetated areas, in addition to commonly used indices like Normalized difference vegetation index (NDVI) and its derivatives, indices that differentiate soil surfaces should also be used (Barati et al., 2011).

### 3.3 Ancillary Data

As topography defines the position of treelines, in addition to satellite data, topographical data were used for determining the ATE. ASTER GDEM (NASA, 2019) was selected to use as the digital elevation model because of its resolution of 30 m, wide accepted usage, and easy accessibility.

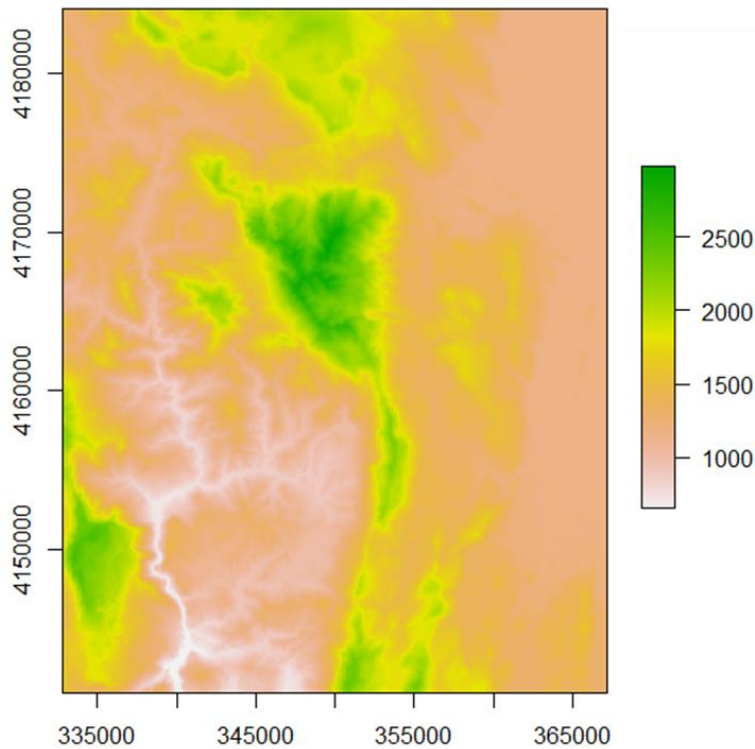


Figure 3.5. Digital elevation model of the Dedegöl Mountain study area

Other topographical data were also derived from the digital elevation model. Slope, slope aspect, topographic roughness index (TRI), and topographic position index (TPI) were calculated using the terrain function of the R package “raster” (Hijmans, 2020). The slope aspect layer was further processed to generate northness and eastness layers, using the R programming environment, using the below equations.

$$\text{northness} = \cos(\text{aspect})$$

$$\text{eastness} = \sin(\text{aspect})$$

Topographic wetness index (TWI) is calculated using the “RSAGA” package (Brenning et al., 2018)

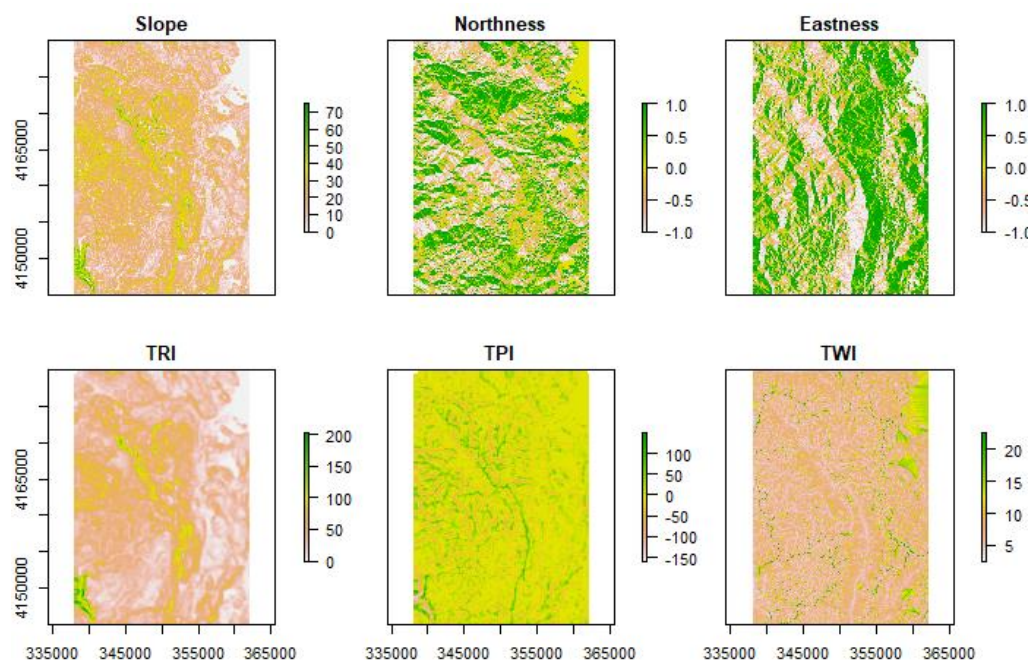


Figure 3.6. Derived topographical layers

Topographic variables were calculated using different spatial resolutions in order to provide the relevant inputs for the model of ATE. Used resolutions are shown below (Table 3.2).

Table 3.2 Topographic variables and calculation scales

Name of the variable	Pixel aggregation	Spatial resolution for calculation
DEM	1	30 m
Slope	1	30 m
Northness	1	30m
	6	180 m
Eastness	1	30m
	6	180 m
TRI	6	180 m
TPI	8	240 m
TWI	1	30 m

## CHAPTER 4

### ALGORITHM FOR DELINEATION OF THE ATE

#### 4.1 Summary of the Algorithm

The flowchart of the algorithm is given in Figure 4.1.

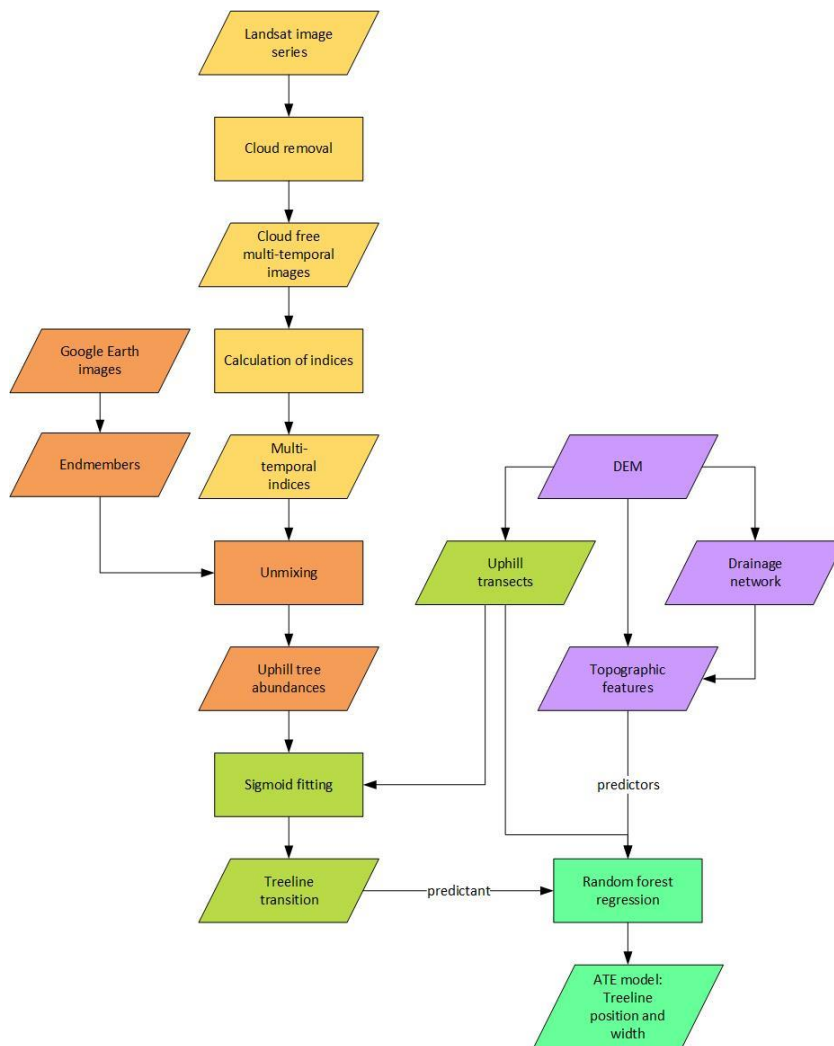


Figure 4.1. Summary of the flow of the algorithm

## **4.2 Cloud removal and calculation of indices**

### **4.2.1 Cloud removal**

With the intention of capturing the temporal characteristics of the area, multi-temporal images were used. Seasonal composites were created to overcome the limitation caused by Landsat's relatively low temporal resolution.

Tree species that live about the treeline are primarily conifers; therefore, the most apparent seasonal change at the treeline ecotone is the change of herbaceous vegetation. Also, since the study area is high altitude, seasons tend to differ from those used in remote sensing analyses, such as agricultural studies. For this reason, the seasons should be selected in order to represent the growing season of herbaceous vegetation present at high altitudes.

By observing the satellite images of the area, the year was divided into four seasons. April-June, July-August, September-October, and November-March.

As mentioned previously, one year's remotely sensed data may not be sufficient to provide cloud-free images that represent each season for some years. Since this thesis aims to develop an algorithm that can be implemented for any year and region, to eliminate the cloudy pixels of Landsat data, an existing study (Man et al., 2018) was simplified and used. This method takes RS images from the previous and following years into consideration, where data from the year of interest is not sufficient.

A procedure was established to overcome the cloudy pixels problem. Firstly, the period to be used for the target year was specified. For example, the three-year period for 2018 means that images from 2017, 2018, and 2019 were used.

Secondly, using Google Earth Engine, the following steps were implemented:

- Images that have less than 10% cloud cover were imported for the selected years.

- Cloud score was calculated for each image using “Landsat.simpleCloudScore” function of the Earth Engine (Gorelic et al., 2017) and added to the image as a band.
- The resulting images were downloaded.

Lastly, the following steps were implemented using R programming environment:

- Year score was calculated for each image using the following formula:

$$yearScore = 1 - |targetYear - imageYear| * \frac{2}{period + 1}$$

- Using the cloud score band and the year scores, a compound weight band was calculated for each image, with the following formula:

$$weightBand = yearScore * (1 - cloudScore)$$

- For each season, bands of the corresponding images were combined using “weighted.median” function of the package “spatstat” (Baddeley et al., 2015).

The year score assigns less importance to the image in hand, as the year of the image used moves farther from the target year, and the cloud score represents each pixel's cloudiness for an image. Combining these two scores enables to assign a measure of quality for each pixel of the images of interest and, thus, provides the most suitable pixels to use for building the seasonal composite image.

For the study area, Dedegöl Mountain, cloudless images were created for 2018 (using images from years 2017, 2018, and 2019) and for 1984 (using images from years 1984, 1985, and 1986). Images from a period of three years were sufficient for cloud-free image calculation of both years.

#### **4.2.2 Calculation of indices**

NDVI, EVI2, NDSI, and NDWI were calculated using the seasonal cloud-free composites. The following formulas were used:

$$\text{NDVI} = \frac{\text{NIR} - \text{RED}}{\text{NIR} + \text{Red}}$$

$$\text{EVI2} = 2.5 * \frac{\text{NIR} - \text{RED}}{\text{NIR} + 2.4 * \text{RED} + 1}$$

$$\text{NDWI} = \frac{\text{Green} - \text{SWIR}}{\text{Green} + \text{SWIR}}$$

$$\text{NDSI} = 2.5 * \frac{\text{NIR} - \text{SWIR}}{\text{NIR} + \text{SWIR}}$$

### 4.3 Transects for examination of the treeline transition

With the aim of minimizing the need for manual interpretation, a simple method has been developed in order to examine the transition area. For the study area's latitude and for its climate zone, ATE is very coarsely located around 1800 m altitude. To explore the transition zone without the bias of this assumption, very long transects were created along the predicted ATE.

Generation of the transects was realized through the following steps, using R programming and QGIS:

- A contour layer has been generated using the DEM for the area of interest using “rasterToContour” function of the “raster” package (Hijmans, 2020) (Figure 4.2).
- The 1300 m, 1800 m, and 2300 m altitude contours around the mountain were selected manually.
- The 1800 m altitude contour was smoothed using the “smoothr” package in R environment (Strimas-Mackey, 2021). The method for smoothing was selected as "ksmooth", which uses Gaussian kernel regression. The smoothing factor was chosen as 50. Smoothing was done to ensure a more homogeneously directed set of transects, i.e., from the foothills to the top of the mountain (Figure 4.3).
- Using the smoothed line, perpendicular transects were drawn to stretch 1000 m in each direction for every 60 m.
- As the slope of the hills is variant around the mountain, to provide a more standard approach, the lines created were trimmed to be constrained by 1300 m and 2300 m altitudes.



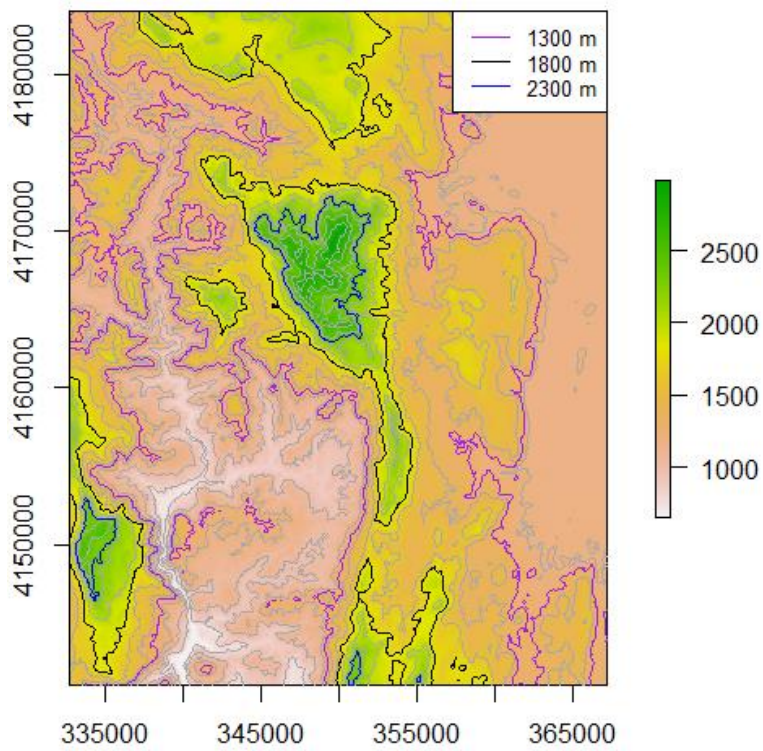


Figure 4.2. Contours on DEM, Dedegöl Mountain

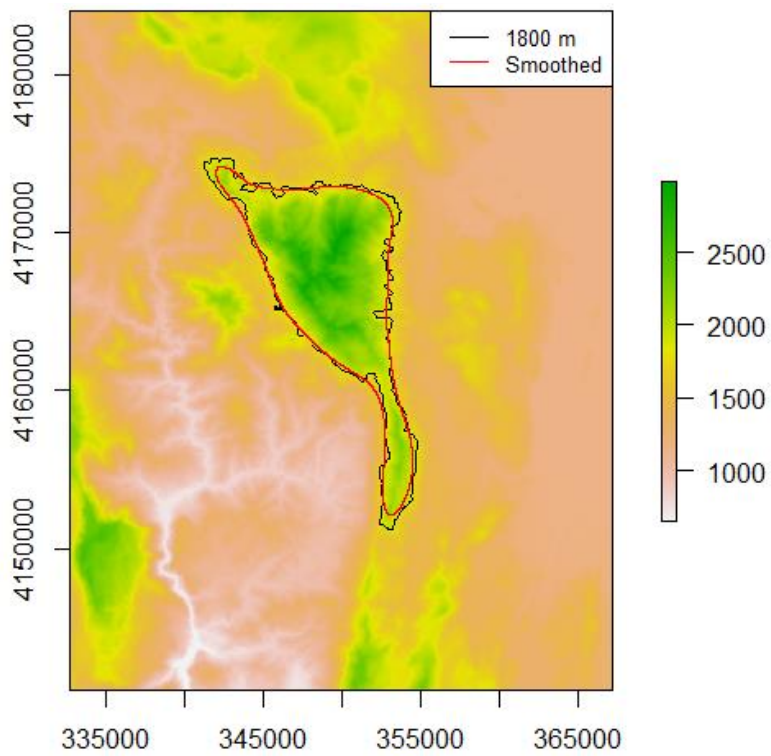


Figure 4.3. 1800 m contour and its smoothing, Dedegöl Mountain

## **4.4 Unmixing using multi-temporal indices**

The main idea is to form multi-seasonal endmembers for main constituents of the ecotone and analyse the transition in terms of the abundances of these constituents.

### **4.4.1 Endmember selection**

Endmembers were chosen to represent the highest abundance in the study area and characterize the ATE transition accurately. As the vegetation cover of the study area consists of coniferous and broadleaved tree and shrub species and herbaceous vegetation, these were chosen as endmembers. Rocks and bare soil, and water were also chosen as the fourth and fifth endmembers to represent non-vegetated areas.

The number of endmembers was deliberately chosen to be a small number. Similar to the situation of unmixing using multi-spectral images as opposed to using hyperspectral images, the input of 16 seasonal indices means high numbers of endmembers must be avoided.

Coniferous tree and shrub species are evergreen and expected to show little variance in terms of reflectance throughout the seasons.

Broadleaved tree and shrub species are mostly deciduous at the study sites. Therefore, they are expected to grow green shoots in spring, have very high NDVI values at the end of spring through the summer, and shed their leaves in autumn.

Herbaceous vegetation, which in the case of mountains are alpine grasslands, strongly reaches its peak of NDVI as the snow cover melts in spring. Then, as the temperatures rise and soil moisture drops, NDVI starts to decrease gradually throughout the summer and autumn. In winter, it is completely covered with snow.

Rocks and bare soil has consistently very low NDVI throughout the year. Soil index and water index only change with the arrival of snow cover.

#### 4.4.2 Unmixing process

The unmixing was done using four indices; NDVI, EVI2, NDSI, and NDWI, for four seasonal composite images. Extraction of these seasonal indices for the endmember polygons resulted in a matrix of five endmembers \* 16 seasonal indices, to be used as the input of the unmixing process.

For performing unmixing, the “mesma” function of the R package “RStoolbox” was used (Leutner et al., 2019). “mesma” stands for multiple endmember spectral mixture analysis, and the function was originally for spectral unmixing. Although indices were used instead of spectral bands in this algorithm, this function was used for unmixing.

The method was selected as NNLS (non-negative least squares) regression which uses SCA (sequential coordinate-wise algorithm) (Franc et al., 2005).

For the scenario in hand, FCLS (fully constraint least squares) is more convenient as the total abundance of endmembers for each pixel is assumed to be 100%. However, as this thesis aims to use open source platforms, NNLS, which is the method available in the R environment, was chosen. To overcome this shortcoming, for calculating the percentage of abundances, the following formula was applied.

$$endmemberAbundance_{[01],i} = \frac{(abundance\ of\ endmember_i)}{\sum abundance\ for\ each\ endmember}$$

#### 4.4.3 Calculation of tree percentage

ATE at the study area consists mostly of conifers, with occasional broadleaved oaks. To consider all of the woody species, the sum of the abundance of the two was calculated using the below formula:

$$treeAbundance = (coniferousAbundance + bradleavedAbundance)$$

This value provides an estimation of crown cover, making it suitable to observe the change through the ATE.

#### 4.5 Fitting of sigmoid waves to the transition of ATE

Using the generated transects, tree percentage values along with the DEM values were extracted, resulting in a plot of tree percentage versus pixel ID. The pixel IDs were sequenced to increase as they moved from the foothill to the top of the mountain. There were small elevation fluctuations since transects are straight line segments, and the topography is not very homogeneous.

Extracted values along the transects were examined, and it is seen that some long transects along the ridge, where the maximum altitude is lower than 2100 m, may reach the max altitude and then start to decrease. Likewise, transects located through a valley may show a trend that decreases first and starts to head up later. To standardize the sigmoid fitting process to the transects, all were examined in the R environment. The line segments were trimmed so that the lines start at the minimum elevation and end at the maximum elevation along the transect.

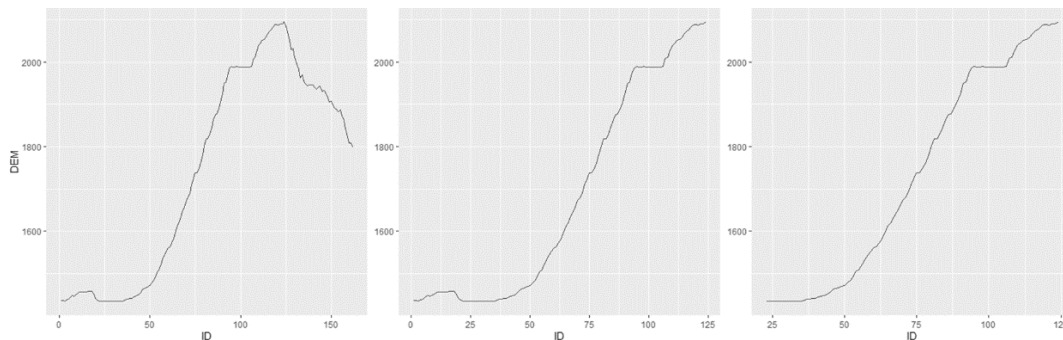


Figure 4.4. From left to right: original transect, part after the maximum elevation was eliminated, the part before the minimum elevation was eliminated.

To eliminate the elevation fluctuations and obtain a monotonically increasing elevation profile, sample points along the transect where elevation drops were not used.

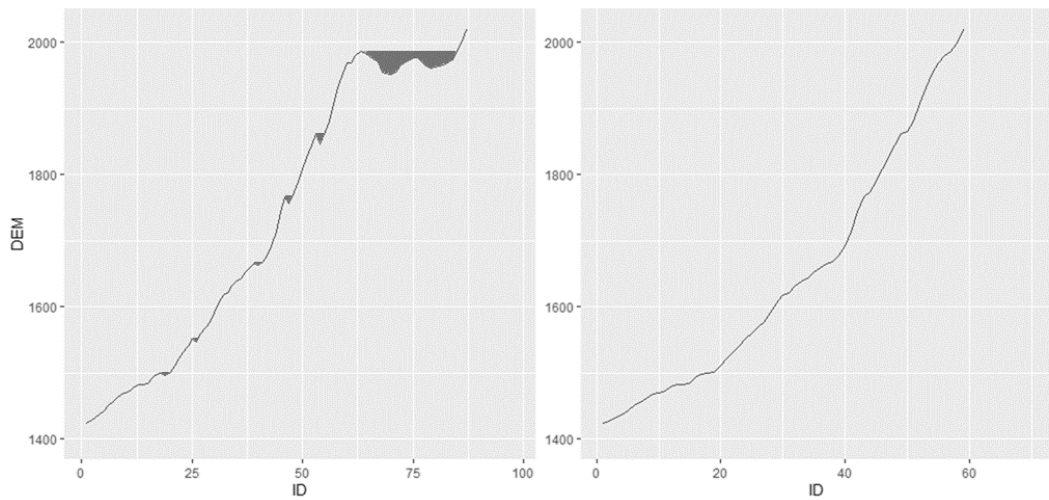


Figure 4.5. An example of before and after the elimination of elevation drops. Filled grey parts were eliminated.

The sigmoid responses were fitted to those plots generated for each selected transect using the “nls” function of R package “stats” (R Core Team, 2020). Not all transects could be fitted since the transition is not always as expected. This situation can be observed where there is grazing or settlement pressure or where a topographic barrier, such as a cliff is present.

To standardize the fitted sigmoids and define the lower and upper limits of the ecotone, the sigmoids were normalized to be in the range [0, 1]. Taking the nature of the sigmoid curve into consideration, the lower limit was defined as 0.9, and the upper limit was defined as 0.1. Also, value 0.5 was defined as the treeline.

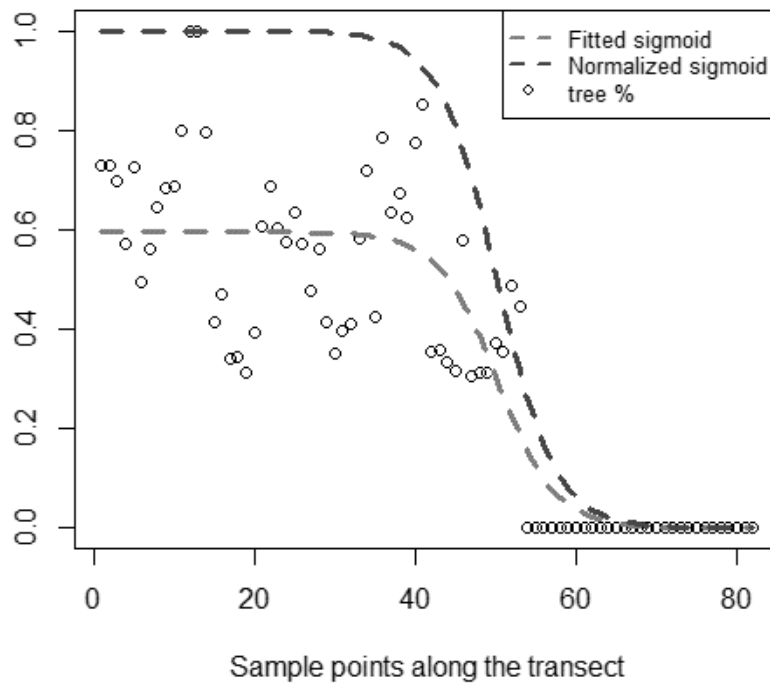


Figure 4.6. An example of fitted sigmoid wave and its normalization

Also, the correlation of the tree percentage values and the fitted sigmoids were calculated for each transect using the “cor” function from the R package “stat” (R Core Team, 2020). Transects that correlate higher than 90% were selected to be used in the training of the model.

As a result of this step, ATE was defined as a transition zone where the sigmoid values represent the nature of the transition at a point.

#### 4.6 Random Forest Regression and Model

In order to model the position of the ATE as a transition zone, firstly, the model was trained using random forest regression.

As predictors, the following topographic variables were used;

- DEM
- Slope

- Northness (two different scales)
- Eastness (two different scales)
- Topographic position index (TPI)
- Topographic roughness index (TRI)
- Topographic wetness index (TWI)

Selected transects to which sigmoids were fitted with high correlation have been used to prepare the predictand input. Along these transects, predictor values and the normalized sigmoid value that represents the ATE were extracted using the “ExtractAlongTransect” function of the R package “inlmisc” (Fisher, 2020). By merging these values, a large matrix of eight variables and 37039 rows was obtained (Table 4.1).

Table 4.1 First ten rows of the matrix for the model input, for Dedegöl Mountain.

DEM	Slope	Northness	Eastness	North_180	East_180	TRI	TPI	TWI	sigmoid
1332.4	15.92	0.925	0.380	0.887	0.462	16.76	3.72	3.238	1.000
1340.4	18.82	0.919	0.394	0.886	0.463	18.98	5.88	3.351	0.974
1349.4	22.69	0.917	0.400	0.881	0.471	20.56	8.04	3.506	0.946
1356.3	26.37	0.876	0.482	0.897	0.440	21.20	11.28	3.400	0.916
1369.5	27.64	0.843	0.538	0.885	0.465	22.20	13.84	3.389	0.884
1383.4	26.94	0.813	0.583	0.877	0.479	23.24	16.40	3.348	0.850
1394.6	28.88	0.845	0.535	0.875	0.484	24.32	18.96	3.402	0.813
1411.3	30.19	0.869	0.495	0.872	0.489	25.13	21.51	3.358	0.776
1423.2	28.80	0.865	0.501	0.869	0.494	25.68	24.24	3.500	0.736
1439.7	27.01	0.886	0.464	0.861	0.508	25.72	27.13	3.417	0.696

The data were randomly divided into two parts for validation; training data to be 80% and test data to be 20% of the original data.

Using the “randomForest” function of the “randomForest” package in the R environment, the model was trained using the following model parameters:

x = training data predictors (First 7 columns of the matrix)

y = training data predictand (Last column of the matrix)

mtry = 3 (Number of variables to be sampled at each split)

ntree = 200 (Number of trees to grow)

importance = TRUE (Importance of predictor variables is to be calculated)

xtest = test data predictors (First 7 columns of the matrix)

ytest = test data predictand (Last column of the matrix)

To run the model for the whole coverage of the area of interest, a raster stack composed of the predictor layers was created. The random forest regression output and the predictor raster stack were used as input to the model using the “predict” function of the “raster” package of R (Hijmans, 2020).

Since the predictand input of the model was the sigmoid values, which changed in the range [0, 1], the output was a raster with values changing from 0 to 1. As stated earlier, the treeline ecotone was defined as the transition zone between the values 0.9 and 0.1. In addition, the treeline was defined as threshold 0.5. The following steps were realized to provide an output that can be easily interpreted.

- Contour lines were drawn for the values 0.1, 0.5, and 0.9 using “rasterToContour” function of the “raster” package (Hijmans, 2020).
- Using those lines, polygons that represent areas corresponding to the values [0,0.1] (area above the upper limit of treeline ecotone), [0,0.5] (area above the treeline), and [0,0.9] (area above the lower limit of treeline ecotone) were created.
- For all three polygons, those with areas smaller than 0.1 km<sup>2</sup> were deleted, and voids smaller than 0.1 km<sup>2</sup> were filled.
- By selecting the [0,0.9] polygons that have [0,0.1] polygons inside, areas that have a complete treeline transition were obtained.
- The same selection was performed for the [0,0.5] polygon.
- By subtracting the [0,0.1] polygons from selected [0,0.9] polygons, the ecotone was obtained.
- By converting the selected [0,0.5] polygon to line, the treeline was obtained.



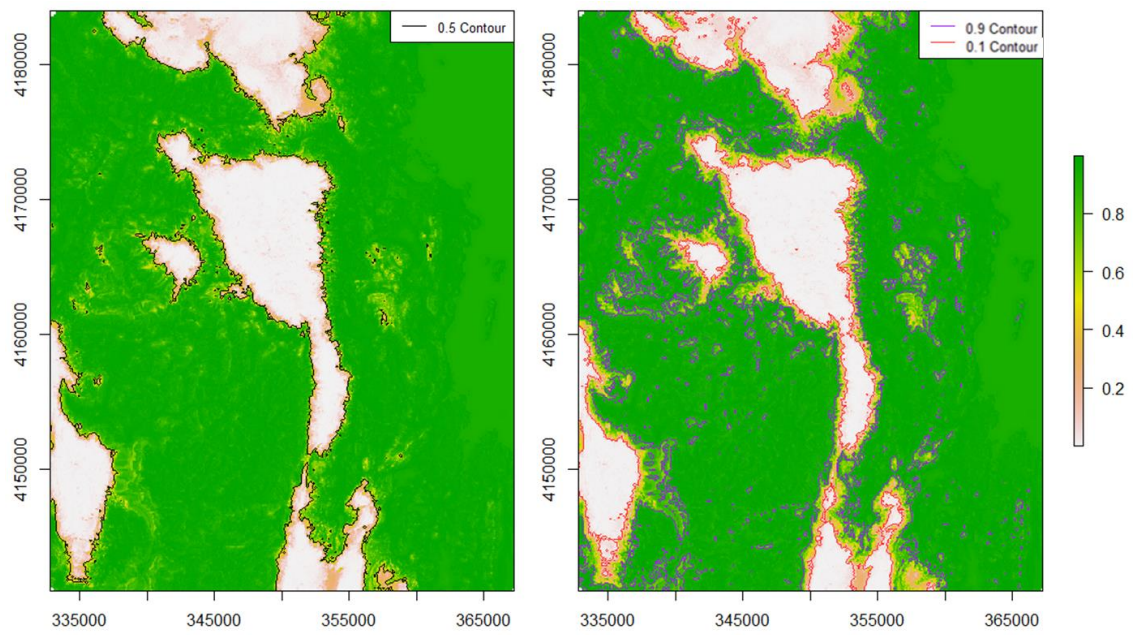


Figure 4.7. The output of the random forest regression, 2018, Dedegöl Mountains



## CHAPTER 5

### RESULTS AND DISCUSSION

#### 5.1 Outputs of the Algorithm

##### 5.1.1 Cloud removal and calculation of indices

###### 5.1.1.1 Cloud removal

An automated cloud removal step is essential for an algorithm that aims to be objective and repeatable. The method developed is fast and easy to implement using Google Earth Engine and R programming platform. This method makes up for periods where cloud-free images are not available by using successive years. Since mountains are areas where gaps in availability of cloud-free images is a frequent problem, this advantage becomes invaluable. In addition, it is possible to standardize the method for any year by predefining the periods for the composite images to be used. Lastly, for satellite images with more than one tile, sometimes partial images of the area of interest are available. This method makes use of partial images by ignoring the NA pixels and using the rest. This feature of the method provides more input to obtain cloud-free images.

Using three successive years' data, cloud-free images were obtained for the study area for 2018 and 1984 years. The improvement can be seen in the images below, showing the cloud-free outputs for the year 2018, calculated using 2017, 2018, and 2019 Landsat images (Figure 5.1, Figure 5.2, Figure 5.3, Figure 5.4).

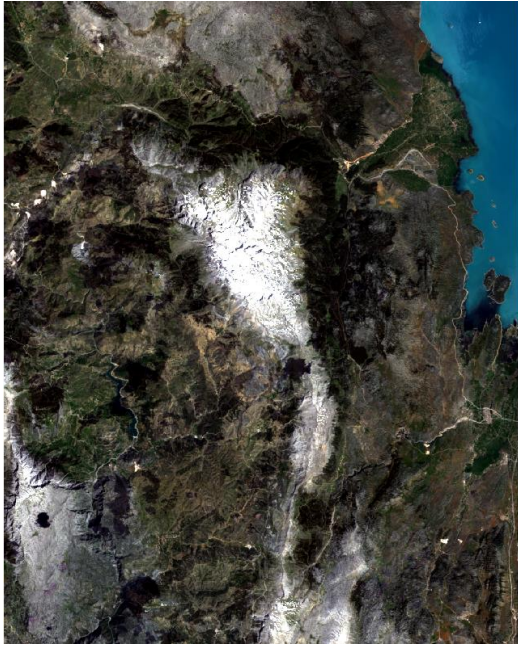


Figure 5.1. Cloudless April – June image for 2018, Dedegöl mountain



Figure 5.2. Cloudless July – August image for 2018, Dedegöl mountain



Figure 5.3. Cloudless September – October image for 2018, Dedegöl mountain

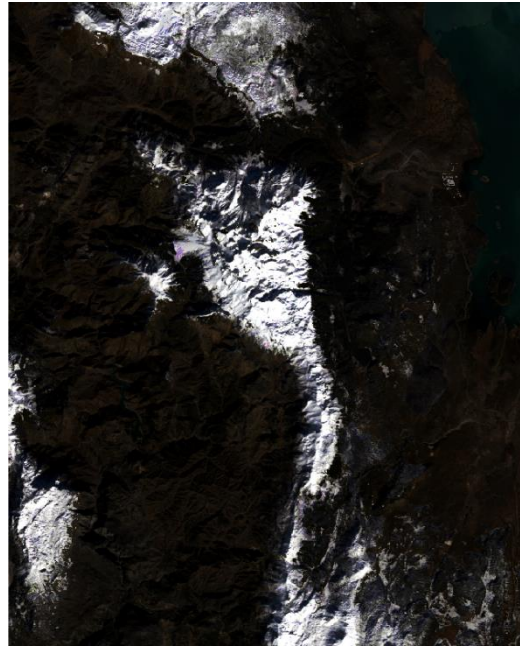


Figure 5.4. Cloudless November – March image for 2018, Dedegöl mountain



### 5.1.1.2 Seasonal indices

Seasonal indices were generated using cloud-free seasonal images calculated for the same period.

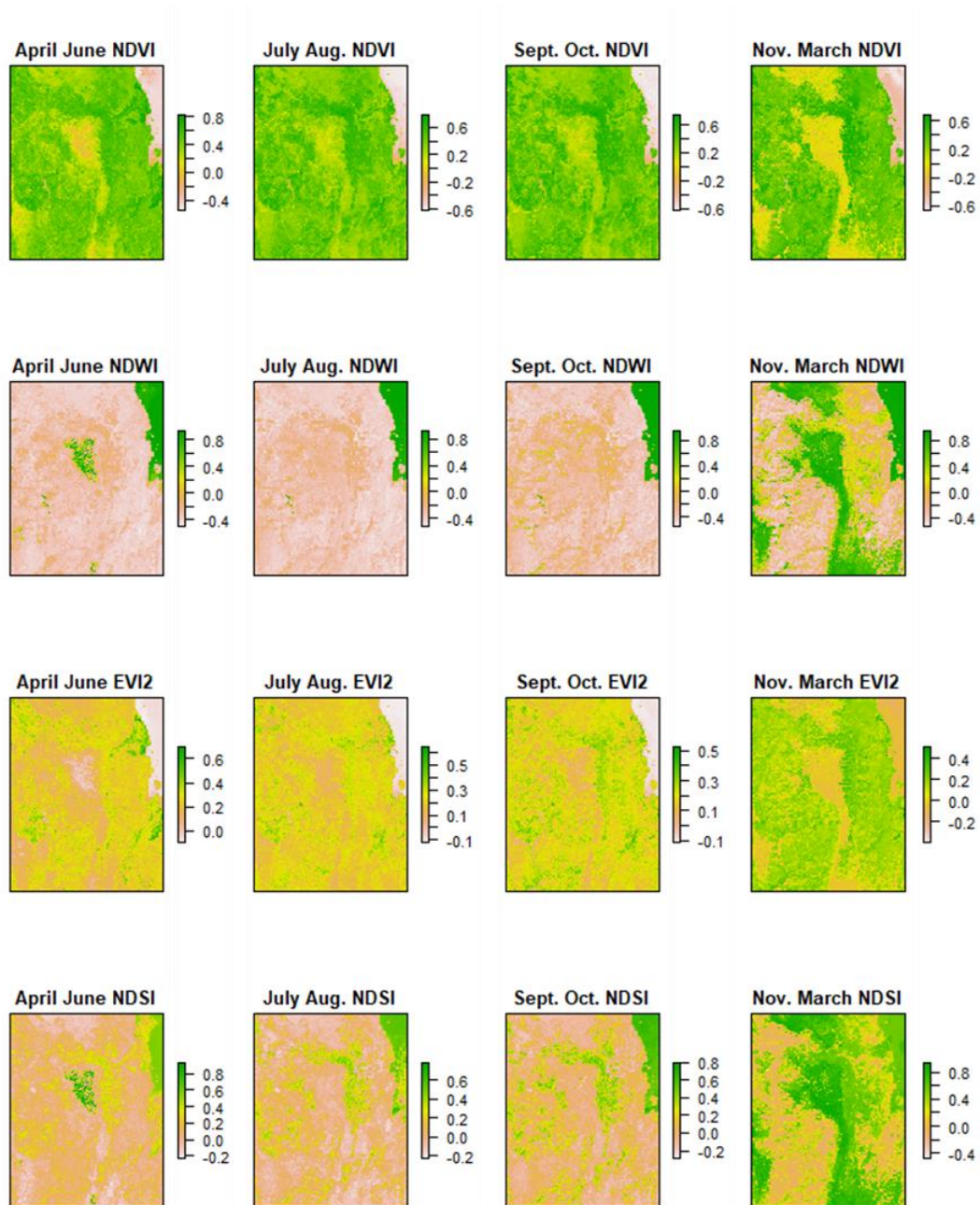


Figure 5.5. Seasonal indices calculated for 2018, Dedegöl Mountain

When correlations are examined, it can be seen that (Figure 5.6) some indices are highly correlated when considered as a whole. Nevertheless, taking into consideration that differences at small areas would be significant for the next steps of the algorithm, no indices were disregarded.

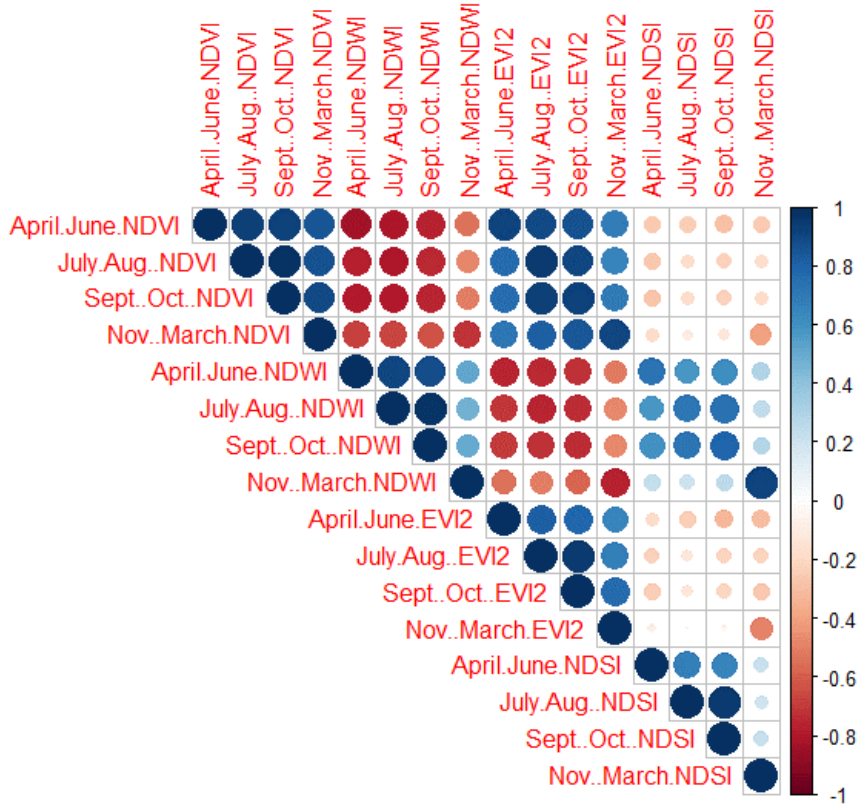


Figure 5.6. Correlation of indices

### 5.1.2 Transects

During the development of the algorithm, the importance of how the transects were drawn was observed. In the early stages of the study, the contour of 1800 m was used directly for the generation of transects. The desired direction of the transects is from downhill to the top of the mountain. However, since the contour is wavy in its nature across valleys and ridges, and the transects were drawn perpendicular to this line, the

process resulted in some transects that were not in the required direction or crossing each other. With the smoothing step added, this problem was solved.

In addition, since the number of transects needed is very high, the advantage of using RS data has become evident.

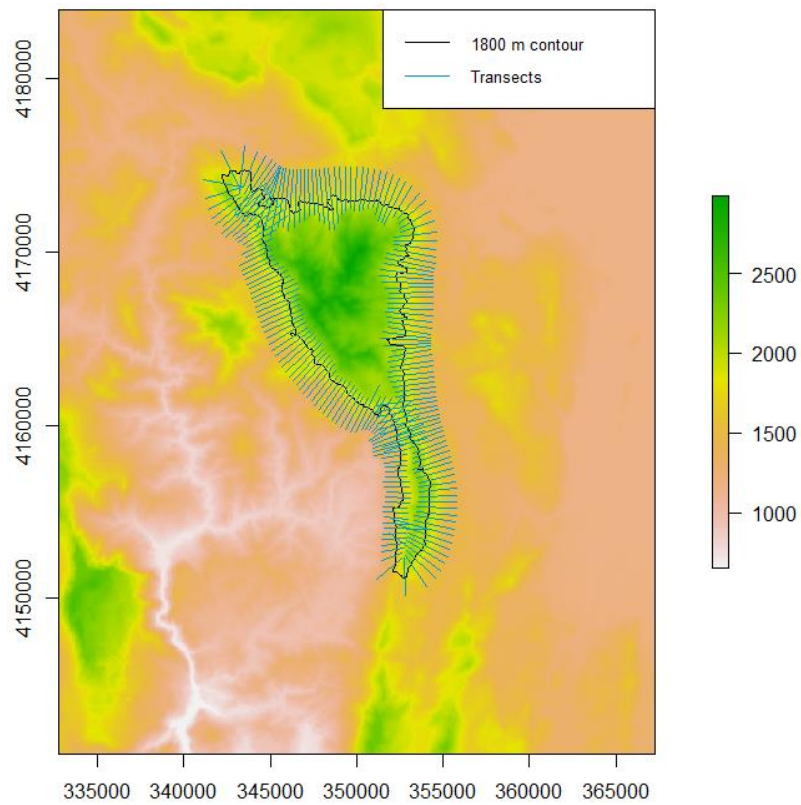


Figure 5.7. DEM, 1800 m contour and transects for the Dedegöl Mountain

### **5.1.3 Unmixing**

#### **5.1.3.1 Endmember selection**

Endmember selection for unmixing was done in order to obtain total tree abundance over the study area.

Broadleaved species that are present in the study area are deciduous or evergreen. Kermes oak is the most widely distributed of broadleaved species at Dedegöl Mountain and its surrounding area, and it is an evergreen species. One shortcoming of this step is that broadleaved trees were not separately examined as deciduous and evergreen species since they are not easily distinguished from Google Earth images and are usually sparsely distributed over the area. Thus, creating pure endmember samples for evergreen broadleaved species was not possible for the study area.

Another limitation was that it was not possible to provide information on the form and height of woody species for the endmember selection process, even though they are important parameters for defining the treeline. Tree species in the shrub form or irregular forms, or smaller trees were not sampled as separate endmembers.

Thirdly, 30 m wide plots of plain pure rock or bare soil are not typical in nature. Even though the endmembers were selected so that the pixels would be as pure as possible, there would be some vegetation present in them.

Endmembers and variations of index values through the seasons can be seen in the figures below (Figure 5.8, Figure 5.9, Figure 5.10, Figure 5.11).

NDVI variation of rocks and bare soil shows that a mixture of vegetation is present at the endmember samples. However, it can be easily distinguished from the other endmembers by observing seasonal changes. Herbaceous vegetation is found in different densities, and this can be observed at the endmember variabilities within each season, especially in the spring. For trees, it can be seen that the variation through seasons is affected by the presence of sparsely distributed evergreen oaks in broadleaved trees samples. Water is easily differentiated for all seasons.



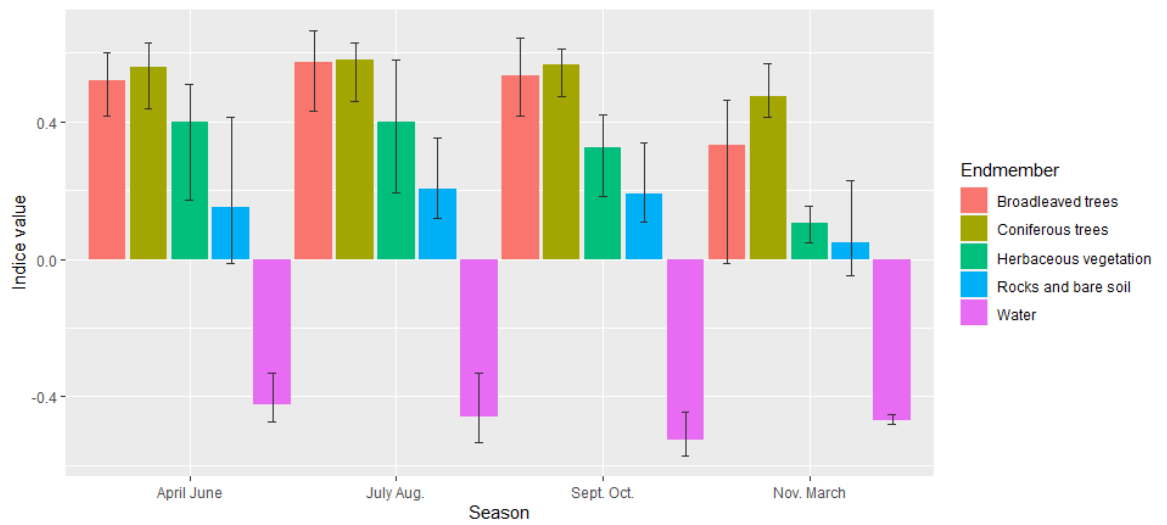


Figure 5.8. NDVI variation through seasons for endmembers

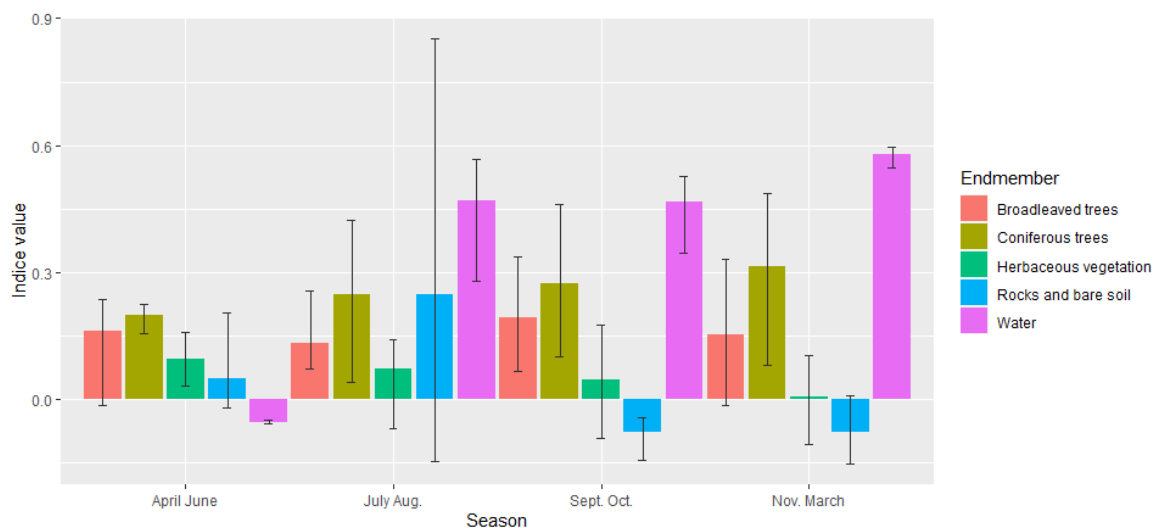


Figure 5.9. EVI2 variation through seasons for endmembers

The high index value of the Rocks and bare soil endmember in summer indicates that after the snow melts, alpine vegetation with a short lifespan emerges strongly at the sample points. Because the NDVI and EVI2 patterns of the endmembers herbaceous vegetation and show a different trend than patterns of rocks and bare soil, it can be concluded that different vegetation covers are present at those sample

points. Therefore, these two endmembers being unmixed separately is not likely to cause a problem.

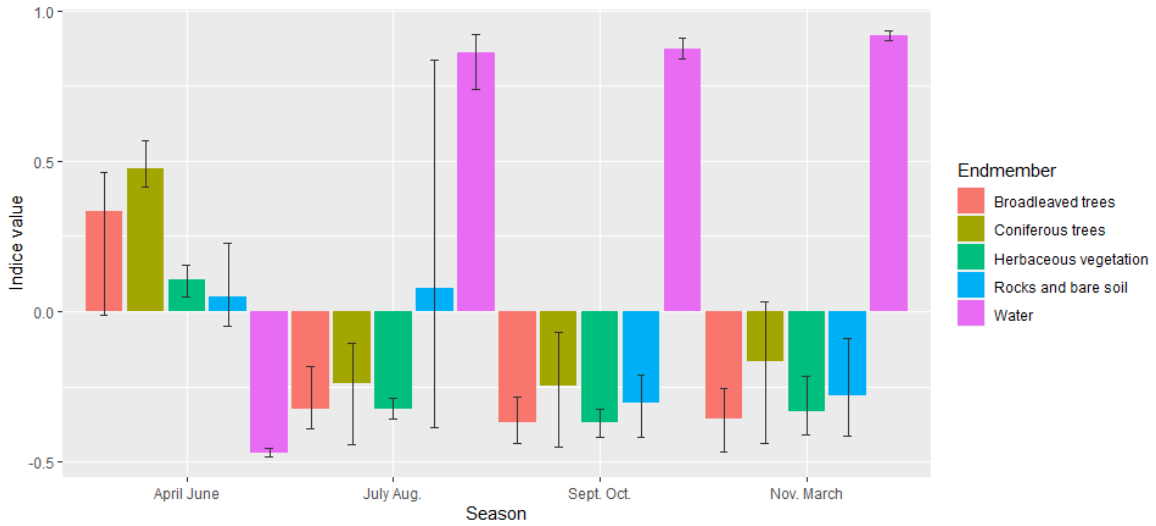


Figure 5.10. NDWI variation through seasons for endmembers

NDWI variation of the tree endmembers through the seasons emphasizes the difference between the broadleaved and coniferous trees.

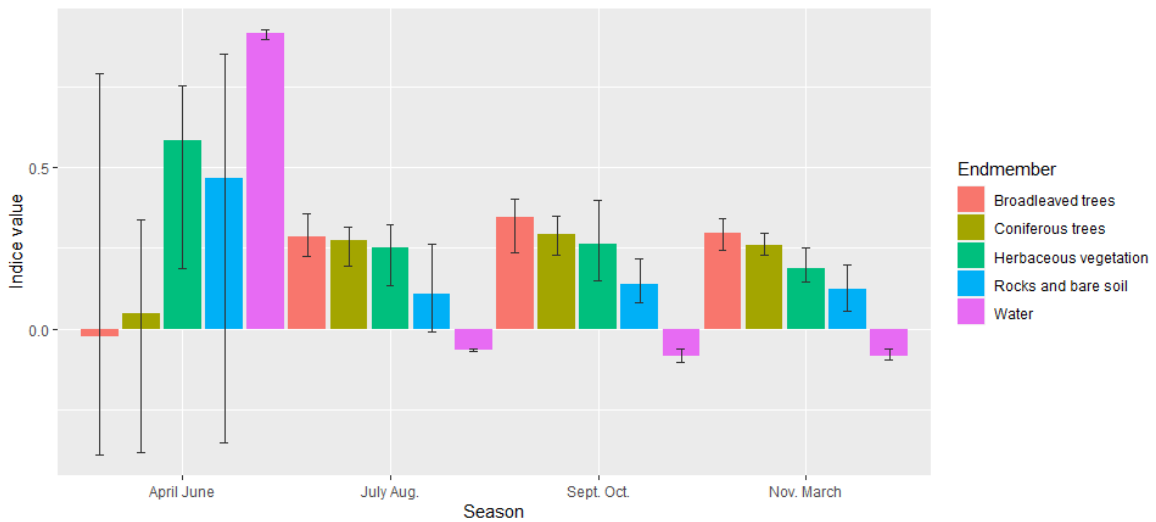


Figure 5.11. NDSI variation through seasons for endmembers

Figure 5.11 shows that the variation within the endmembers in spring is very high. The reason might be the melting of snow cover during those months. Because all

endmember samples are located in various locations in the study area, melting may not occur at the same date. Moreover, the herbaceous endmember has a high value of soil index. This may be caused by newly emerging annual herbaceous vegetation at the time. Another unexpected case present in the plot is that water takes a high index value in spring with a small confidence interval. The water endmember samples were located on the Beyşehir Lake. Although it is not an expected situation as the water level increases as the melted waters emerge to the lake in spring, it may be related to the increase in primary production at those months (Bucak, 2017) and requires further investigation to determine the cause.

Also, another examination was done using the reflectance values of the bands; blue, green, red, NIR and SWIR. This analysis shows that endmembers were not selected from the best sites to represent them Figure 5.12. A more detailed selection process is needed to improve the representations of vegetation and land cover uses in the area.

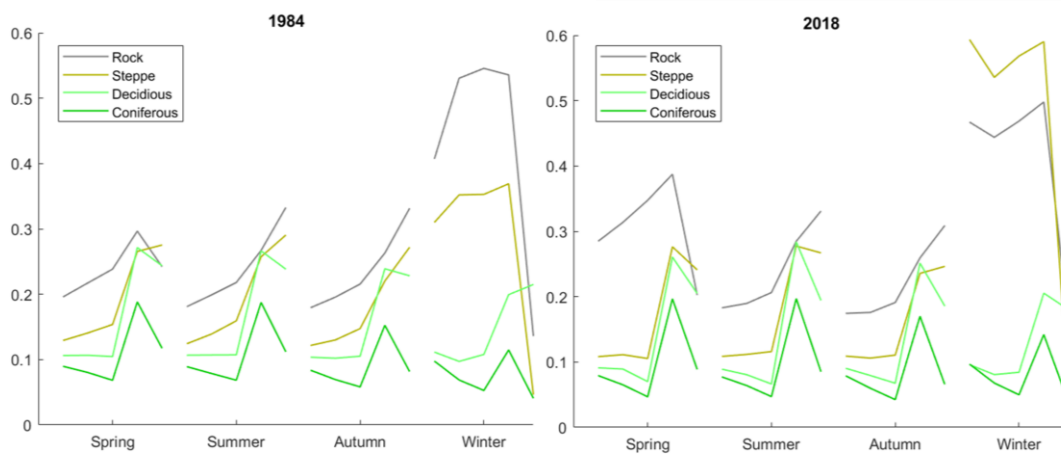


Figure 5.12. Reflectance values of five bands for the endmembers

### 5.1.3.2 Unmixing results

The resulting maps for each endmember and the RMSE are shown below (Figure 5.13 and Figure 5.14).

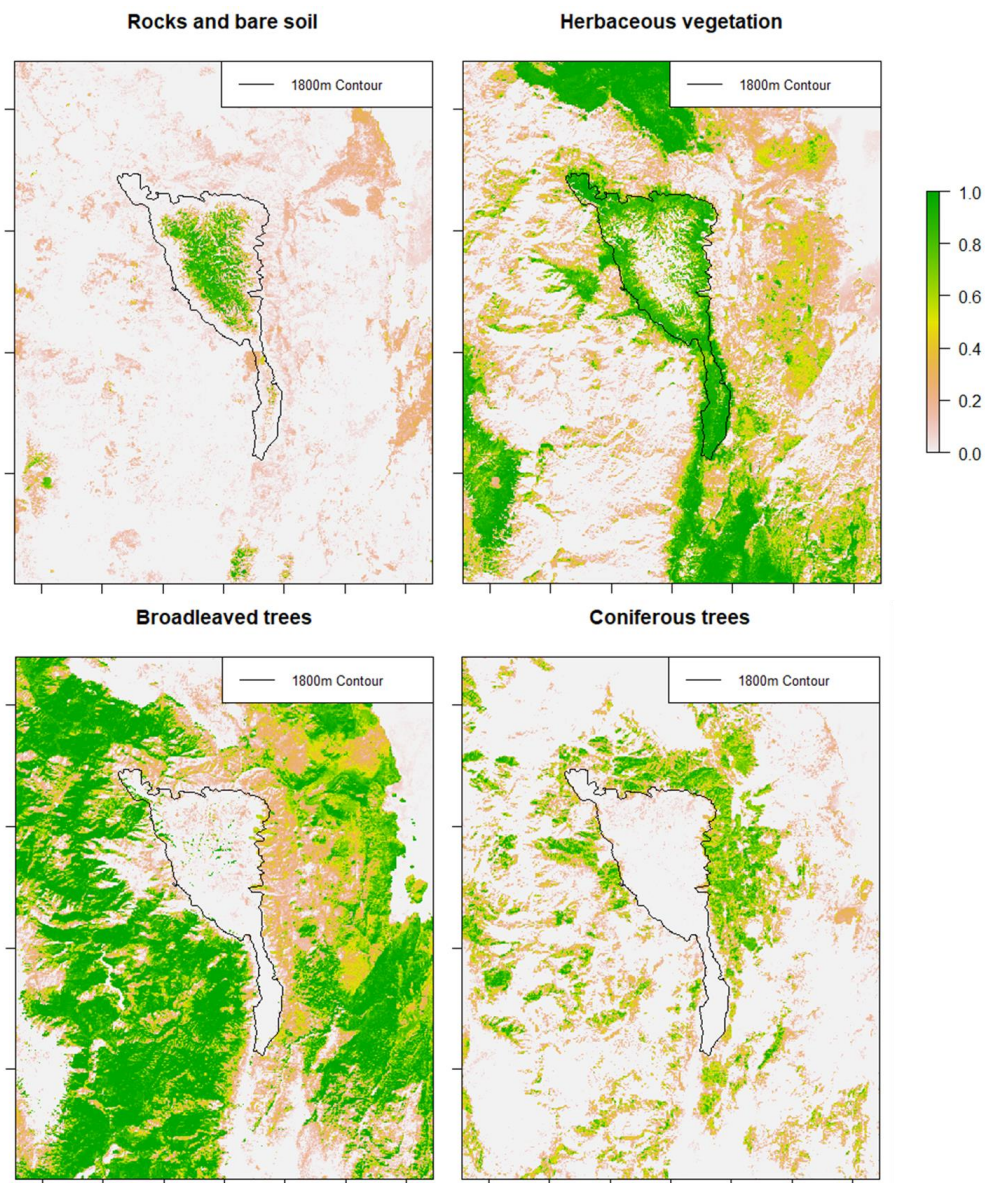


Figure 5.13. Results of unmixing for the endmembers, Dedegöl mountain

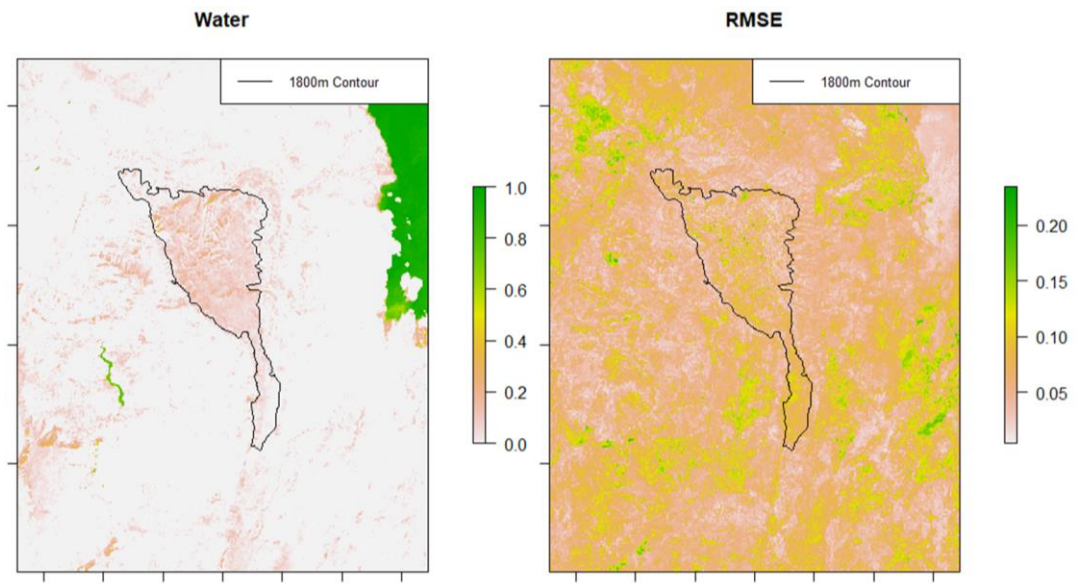


Figure 5.14. Results of unmixing for the endmembers, and the RSME

Evergreen species abundances were classified as conifers or broadleaved trees in the output pixel mixture. However, as the broadleaved and coniferous tree abundances were summed to obtain total tree percentage, this issue did not affect the further steps of the algorithm excessively.

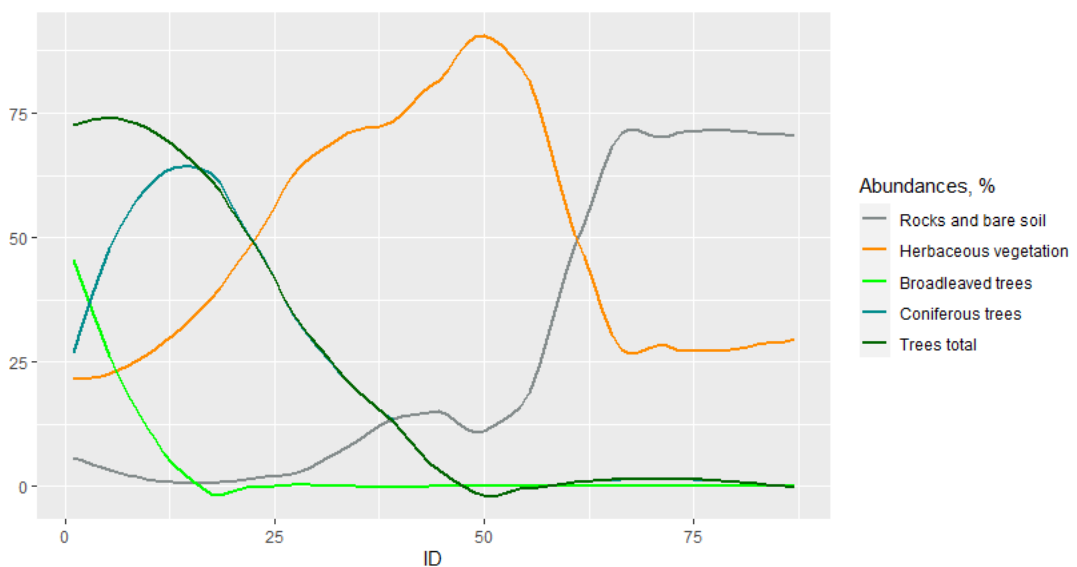


Figure 5.15. Results of unmixing extracted for a transect as an example



Abundances of each endmember change going uphill. Typically, where human disturbance is not high, total tree abundance is higher on the lower slopes of the mountain. This is expected when the dominant ecosystems are forests in the area. When moved upwards, the abundance of trees decreases, and herbaceous vegetation abundances start to increase. This transition is the ATE. Going farther up, the vegetation becomes sparser, and the abundance of rocks and bare soil increases (Figure 5.15).

### 5.1.3.3 Tree percentages

As seen in the figure below, the abundance of woody vegetation, which is shortly referred to as tree percentage, decreases sharply around the 1800 m elevation contour (Figure 5.16). This abundance value is an indicator of canopy cover. Although this value cannot give direct information about the tree height, moving up the treeline ecotone, as the trees get smaller in size, the abundance is expected to get smaller too.

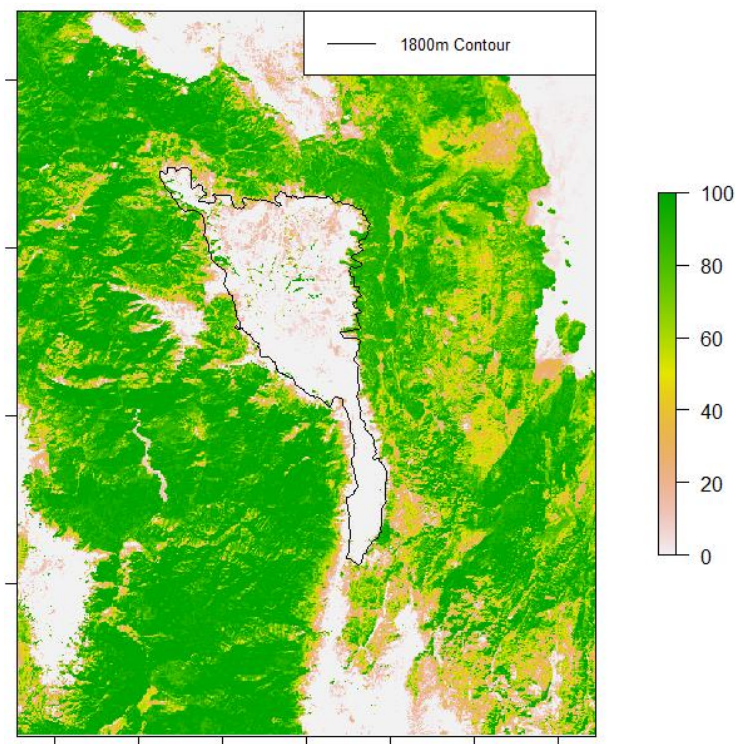


Figure 5.16. Percentage of trees, 2018, Dedegöl Mountain

#### 5.1.3.4 Assessment of the unmixing step

During the unmixing process, normalized difference indices NDVI, EVI2, NDWI, and NDSI were used to overcome the effects of shadows on satellite images. Since this approach is not frequently used, the decision to use the indices has been backed up by comparing the results obtained using these four indices and using the bands' reflectance values (Figure 5.17). Since it is easier to interpret using the tree abundance change, images showing the difference between the 1984 and 2018 images were compared with the help of Google Earth images for visual interpretation. Both approaches, especially unmixing with bands, estimate the tree abundance for the aforementioned years successfully for the areas where the abundance is increased. Unmixing using bands indicates a decreasing trend at and above the treeline at the north and west slopes of the mountain, which does not accurately describe the actual situation. In contrast, unmixing with indices indicates a decreasing trend at and below the treeline, reflecting the actual case more closely but exaggerating the change at the lower flat surfaces. Both models have their weaknesses, but since this output was generated to be used in modelling the treeline, unmixing with normalized difference indices was chosen.

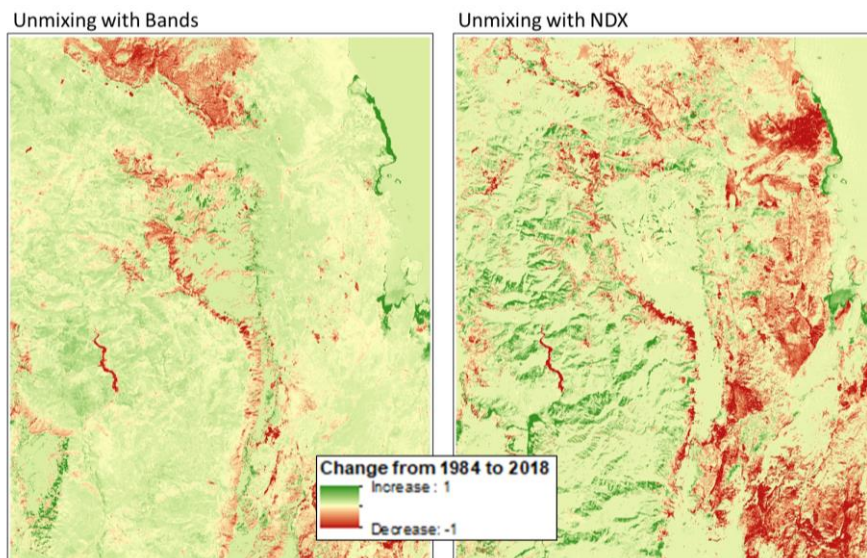


Figure 5.17. Comparison of tree abundance changes from 1984 to 2018, generated using spectral bands and normalized difference indices

Tree abundance and their change maps show that the unmixing approach is more robust for some species. The eastern slopes, which consists mainly of black pines and cedars, is more accurately represented by the output of this step. This may be due to their tendency to form denser forest patches, which can be observed in the study area. In contrast, the west-facing slopes dominated by more sparsely dispersed juniper and oak species, representation success slightly drops.

This step of the algorithm has shown that unmixing of areas where the woody vegetation is sparsely dispersed requires further efforts for the determination of endmember pixels to be used as input for unmixing.

#### 5.1.4 Fitting of sigmoid waves

For 965 transects around the Dedegöl mountain, 669 of them were fitted with sigmoid responses successfully, using tree percentages calculated from the 2018 images of the study area. 455 of those transects were fitted with a correlation higher than 90% (Figure 5.18).

Although climatically suitable, other factors can limit tree growth. Therefore, the transition is often not in a standard form. There may be openings in the forest just below the treeline, or trees may be sparsely distributed at the lower side of the ecotone due to reasons like poor soil conditions or grazing pressure. These cases may cause the sigmoid to fit poorly to the tree abundance samples along the transect.

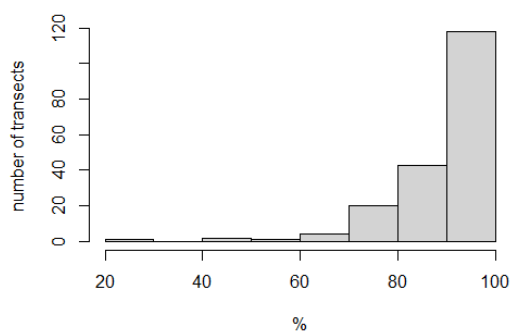


Figure 5.18. Histogram for correlation of sigmoid fits to the tree abundances of input sample points



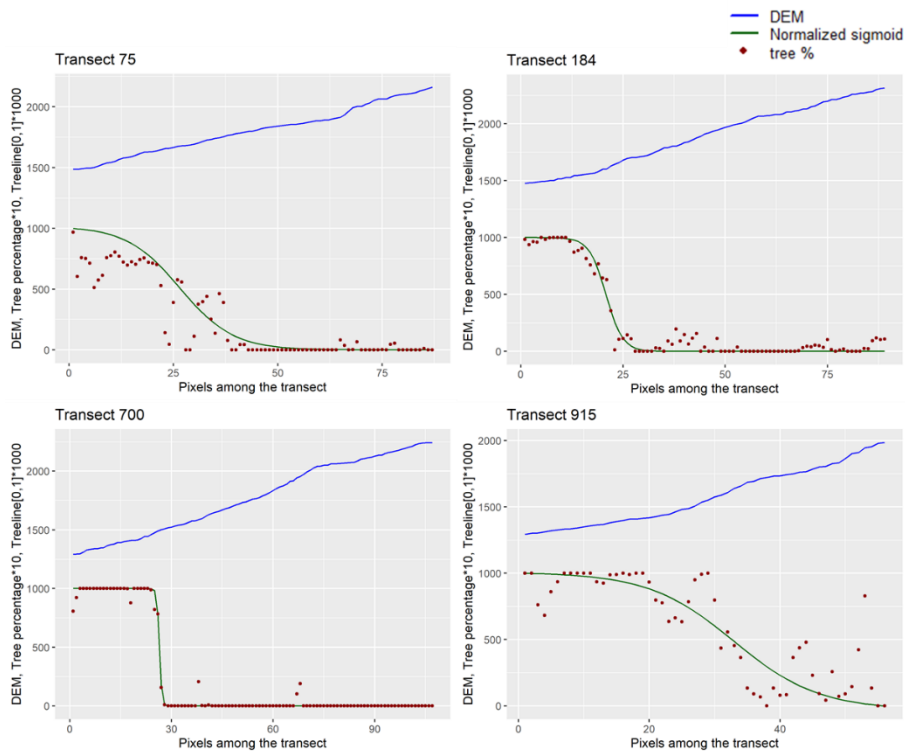


Figure 5.19. Examples of successfully fitted transects (correlation > 90%)

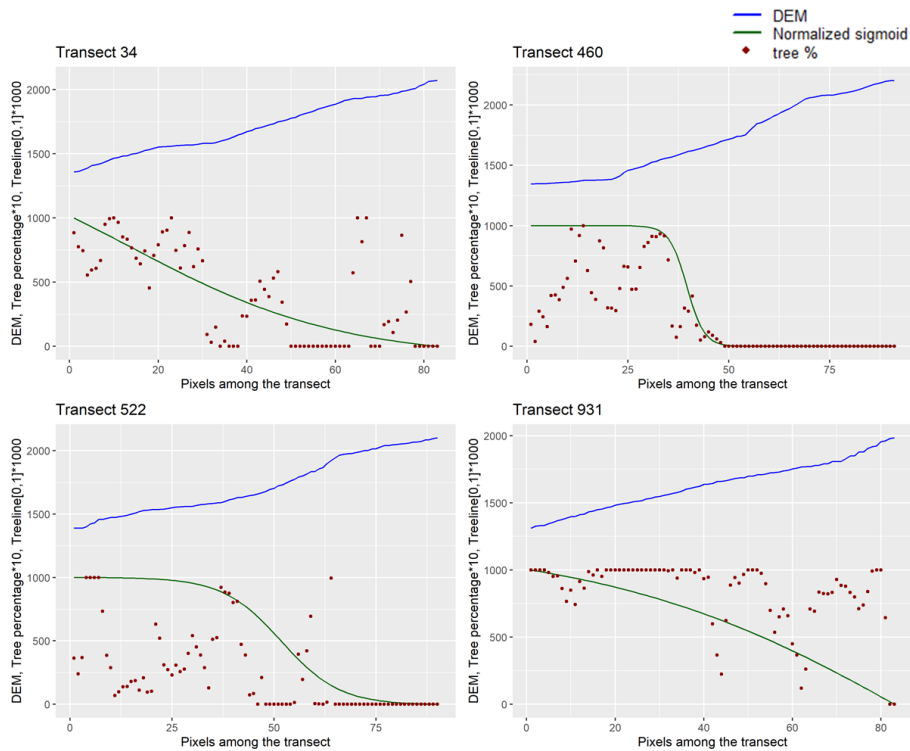


Figure 5.20. Examples of poorly fitted transects (correlation < 90%)

## 5.1.5 Random forest regression and model

Results of the regression and model are examined here in two perspectives; quantitatively and qualitatively.

### 5.1.5.1 Quantitative results

Firstly, the predictor variables' importance and the effect of their addition were inspected. It can be seen that addition of each variable results in a decrease in the error of the regression (Figure 5.21).

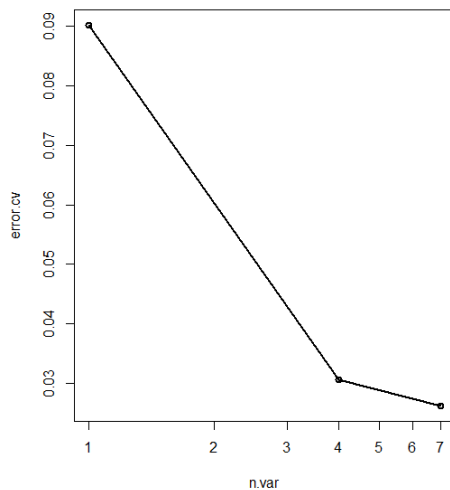


Figure 5.21. Error versus the number of variables for the regression.

Variable importance was also calculated for the regression model. The bar plot below (Figure 5.22) shows the variable importance in terms of mean decrease in accuracy (%IncMSE) and mean decrease in the Gini index (IncNodePurity).

%IncMSE is a measure of comparison between using random values to using values from the variable in question. IncNodePurity is a measure of the effect of splitting. For both variables, higher values mean higher importance (Liaw and Wiener, 2002).

As expected, altitude is the most important predictor. Secondly,

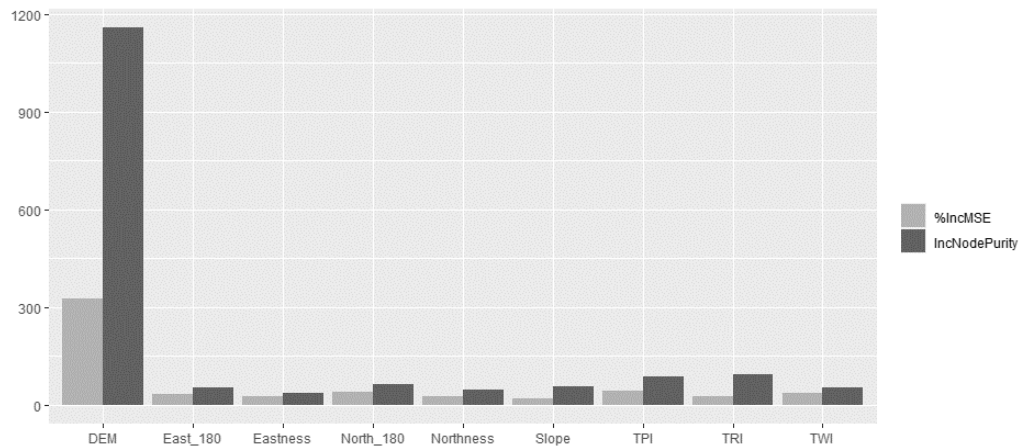


Figure 5.22. Predictor variable importance plot

Accuracies for training and test data are shown below as an output of the regression (Figure 5.23). RMSE is 0.025 for training and 0.02 for test data. The predictand values range from 0 to 1; the regression model can be considered successful regarding the RMSE values. For training data, 88.4% of the variation is explained by the model, and for test data, this value is 88.3%.

```

> print(treeline.rf)

Call:
randomForest(x = traindata[, c(1:7)], y = traindata$sigmoid,
             xtest = testdata[, c(1:7)], ytest = testdata$sigmoid, ntree = 200,
             mtry = 3, importance = TRUE, na.action = na.omit)
  Type of random forest: regression
    Number of trees: 200
No. of variables tried at each split: 3

  Mean of squared residuals: 0.02473755
    % Var explained: 88.4
      Test set MSE: 0.02
    % Var explained: 88.33

```

Figure 5.23. Accuracies of training and test data

### 5.1.5.2 Qualitative results

Visual investigation of the model output shows that the model estimates the actual case successfully for some situations, but for others, there are problems. Examples of successful fits are shown in Figure 5.24 and Figure 5.25.

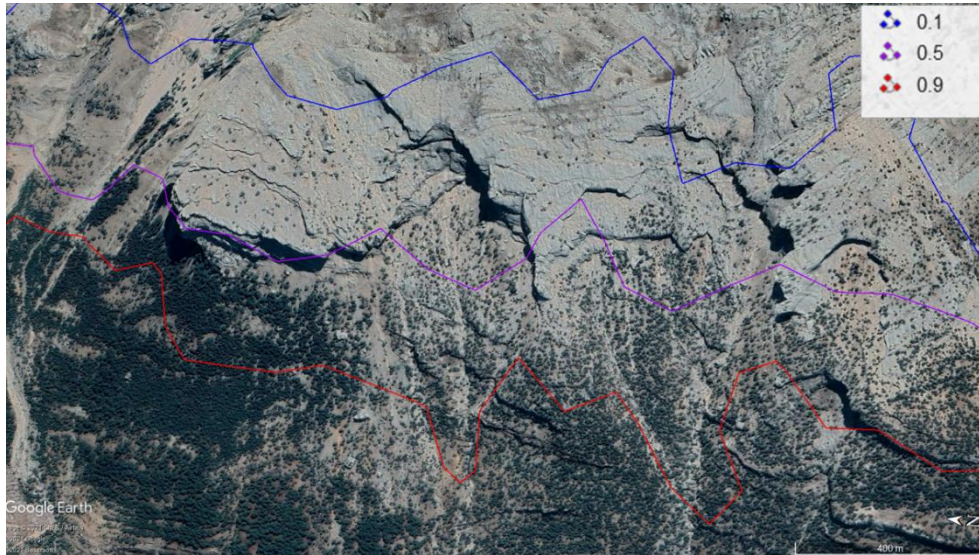


Figure 5.24. An example from model output, calculated using 2018 images, Dedegöl Mountain

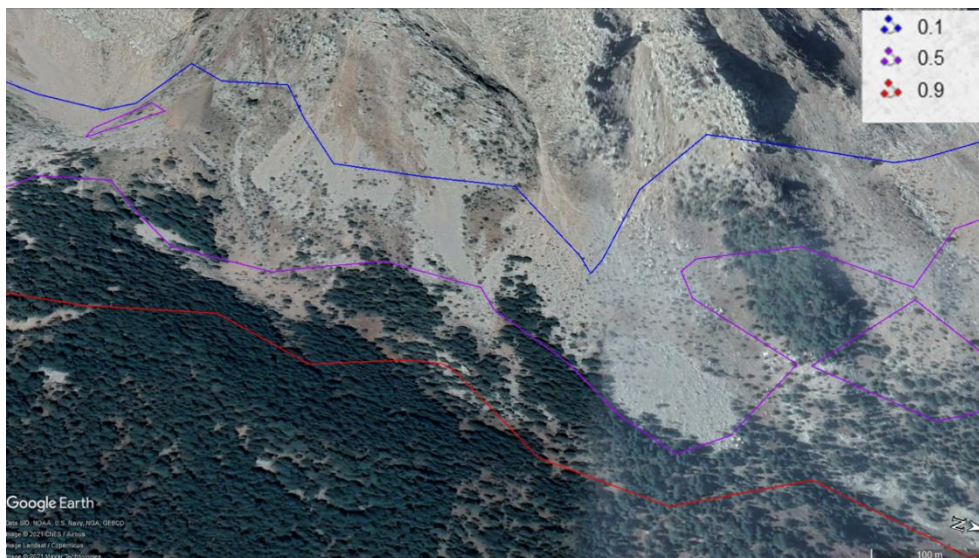


Figure 5.25. An example from model output, calculated using 2018 images, Dedegöl Mountain



In the images (Figure 5.24, Figure 5.25, Figure 5.26, and Figure 5.27), the blue line (0.1) represents the upper limit of the ecotone, and the red line (0.9) represents the lower limit. The purple line is the treeline.



Figure 5.26. An example from model output, calculated using 2018 images, Dedegöl Mountain

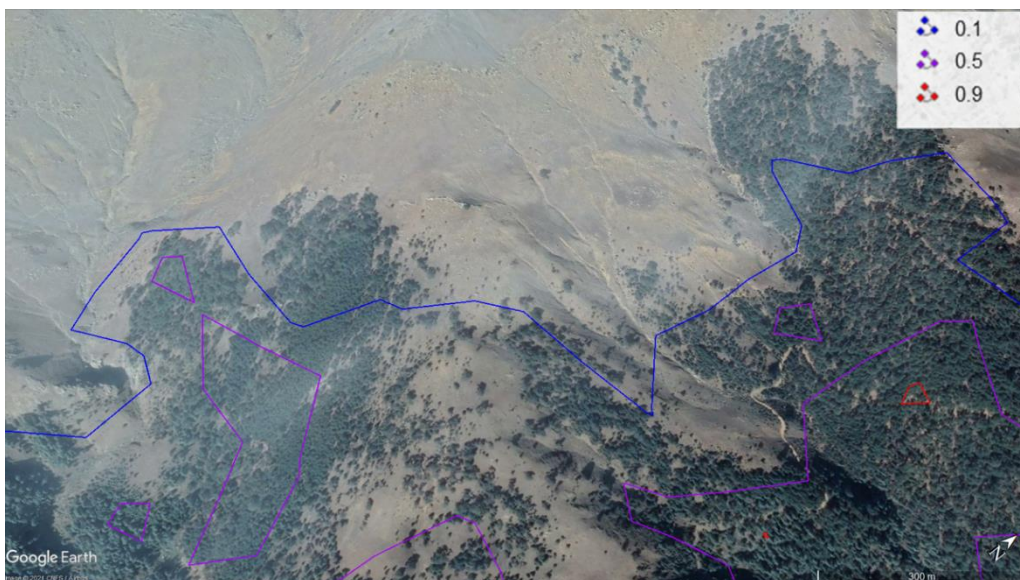


Figure 5.27. An example from model output, calculated using 2018 images, Dedegöl Mountain

For some parts, model estimation fails by extending the upper limit of the ecotone well into openings above forests. Most of the time, this situation is caused by the presence of scree paths. As the model does not use the locations of screes or lithology information, it cannot predict such openings. In Figure 5.26, it can be seen that, although the model predicts that topography is suitable for treeline to reach a higher elevation, scree areas likely prevent that.

For some areas, the actual treeline reaches higher than the predicted line. This may be caused by the microclimate of that specific valley. Such local climate variation cannot be estimated by the model correctly. An example of this situation is presented in Figure 5.27.

#### **5.1.5.3 Assessment of the Random forest regression model**

The high quantitative accuracy of the model verifies that this step of the algorithm provides a robust method for modelling the treeline ecotone using the sigmoids fitted to the tree abundance. The qualitative results show that the model gives valuable results. However, the model failing at occasional areas points to some problematic aspects of the input.

## **5.2 Change of treeline position from 1984 to 2018, Dedegöl Mountain**

Unexpectedly, the model suggests that treeline altitude has dropped for most slopes of the mountain over the 34-year period. The drop can be observed on the west side of the mountain in (Figure 5.28). The drop at this specific slope is due to the tree cover at the ecotone becoming less dense. Thus, change occurs in a longer transect, and the ecotone becomes wider, lowering the midpoint of the transition, which is defined as the treeline.



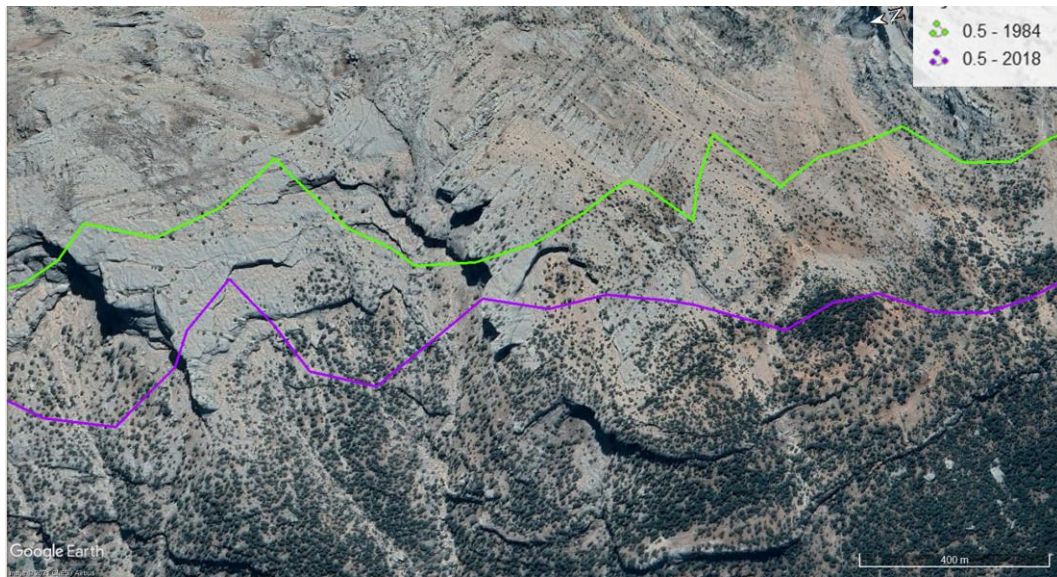


Figure 5.28. Comparison of 1984 and 2018 Treelines, western slopes of Dedegöl Mountain

No significant change can be detected on the northern slopes with occasional increases and decreases (Figure 5.29).

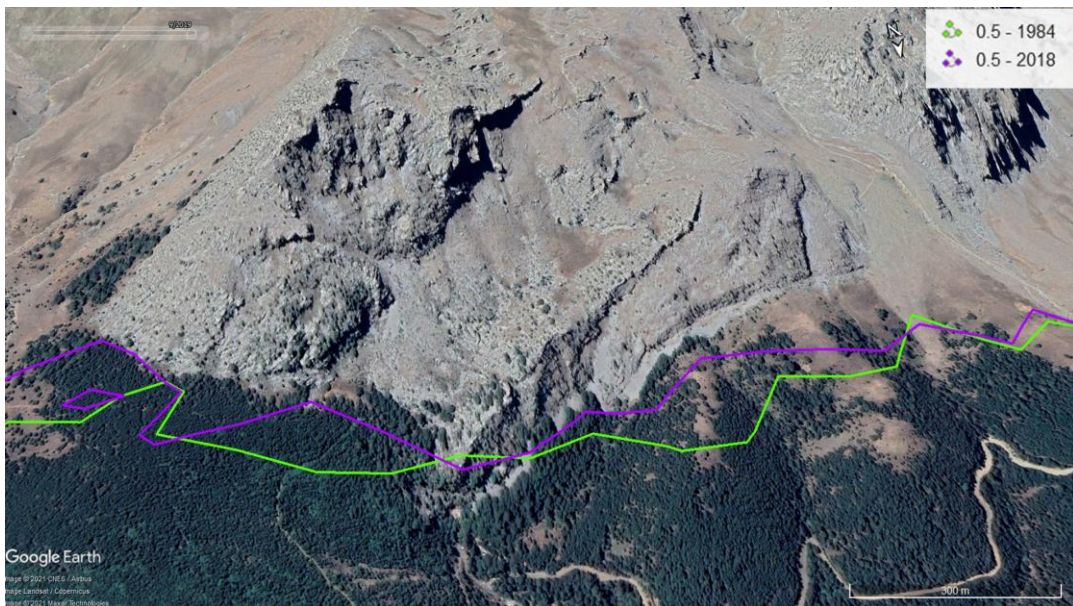


Figure 5.29. Comparison of 1984 and 2018 treelines, north slopes of Dedegöl Mountain.

On the eastern slopes of the mountain, the treeline has not shifted much, although, on some east-facing slopes, an upwards shift can be observed clearly when the upper limit of the treeline is examined (Figure 5.30).

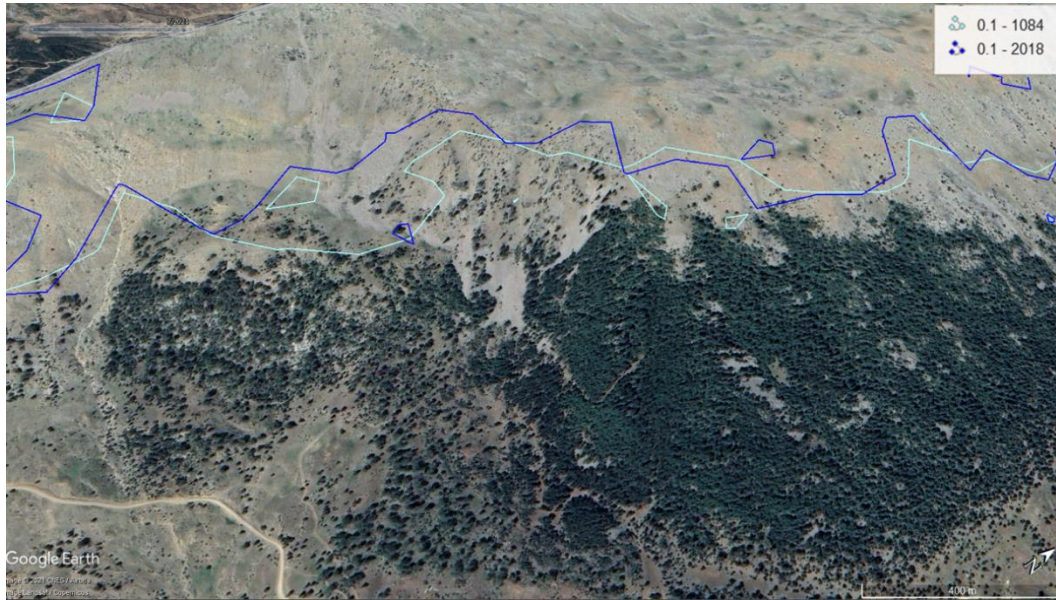


Figure 5.30. Comparison of 1984 and 2018 upper limit of ecotones, east slopes of Dedegöl Mountain.

When the transects that sigmoid curve has been fitted the tree abundance with high correlation are examined, it can be seen that the change in treeline elevations are distributed as follows (Figure 5.31). The mean value for change is a decrease of 22.9 m.



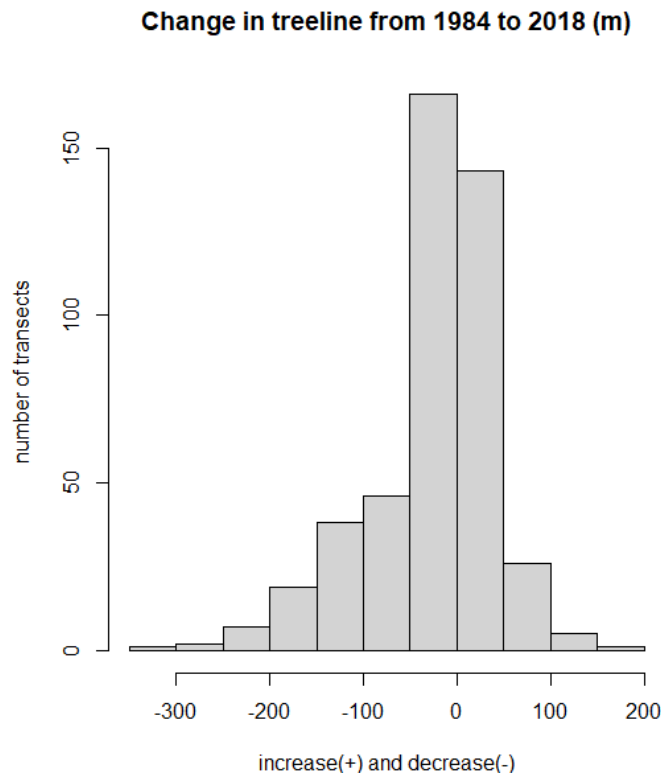


Figure 5.31. Barplot showing the change in treeline altitude

### 5.3 Discussion

The algorithm developed provides more information on the nature of the treeline ecotone at the Dedegöl Mountains at each step of it. Firstly, cloud-free images and normalized indices give an initial idea of the area. Then the unmixing step presents the abundance, which gives an insight into the vegetation cover of the mountain. The addition of sigmoid fitting and the random forest regression model provides an understanding of the factors that shape the treeline ecotone. This last step also gives a tool to model similar areas and estimate the ATE.

The most surprising finding is the lowering of the treeline from 1984 to 2018 at the mountain's eastern slopes. Models are simplifications of the real world, and it is impossible to reflect every aspect of the real world in a model; thus, assumptions are

used to reflect it as efficiently as possible. Simplifications in this model include excluding grazing pressure by domestic flocks and disregarding the complex interaction between temperature and rainfall. Either of those factors might possibly cause a recession of the treeline by lowering the survival and growth of physiologically stressed tree saplings on the ecotone.

Examination of Landsat images and the calculated NDVI maps for both years indicate that as the seasons change with the changing climate, both woody and herbaceous vegetation has become greener in the spring and summer months, and the period that they stay green has increased. This observation emphasizes the need for more complex models to model the ATE that distinguishes the woody vegetation from herbaceous vegetation, than only using NDVI differencing.

Nevertheless, NDVI is a powerful tool that can also be used for visual interpretation. Along with the moderate resolution images, NDVI can give the observer an idea of how the tree cover changes over the years. A visual check of NDVI maps for both years reveals densification of trees across the treeline ecotone for some areas where the model suggests that it has decreased. Further examination of such areas using the tree abundances suggests that the problematic areas are where the unmixing has a poor output.

Since the algorithm was developed in a way that its overall accuracy is the accumulation of each step's accuracy, the model is dependent on the unmixing step. This step may be improved by further efforts and fieldwork, which is beyond the scope of this thesis.

This algorithm cannot take the tree height and the change in form from tree to shrub or krummholz into account. However, this shortcoming was compensated by defining the transition by sigmoid curves and using thresholds to define the upper and lower limits.

The objective for developing this algorithm was to create a method that is ecologically meaningful and easily repeatable. The algorithm developed fulfils this objective.

## CHAPTER 6

### CONCLUSIONS

In a world where climate change is starting to gain unprecedented pace, monitoring its effects on ecosystems is an essential tool for understanding what the future will bring and for sustaining adaptation, mitigation, and conservation attempts. As the climate changes, some indicators of the response of nature can be observed spatially. Forests are the most suitable ecosystems for monitoring this response, as this can be done using remote sensing applications. Ecotones, connecting the forests to other vegetation types, respond to climate change in a way that can be monitored using publicly available remotely sensed data. In addition, ecotones are worth monitoring as they are important areas on their own for biodiversity.

This thesis has developed a reproducible method for monitoring Alpine treeline ecotones, using publicly available data and open source programs. Since Landsat satellites that provide 30 m resolution images of the Earth have been in orbit for nearly forty years, using these images was preferred. Despite their relatively coarse resolution, Landsat images provide invaluable information necessary for analyzing past changes, thus enabling the prediction of future changes. By using unmixing, sigmoid fitting, and random forests regression, the dependency on human interpretation has been minimized.

The output of the algorithm has shown that topographical variables combined with the canopy cover information can be used for effectively modelling the treeline ecotone. The model indicated the treeline had shifted downwards since 1984 at the western slopes of the Dedegöl Mountain, against theoretical expectations or contrary to observations of increases elsewhere in the world. On the eastern slopes, the shift is indicated to be upwards.

This study can provide input for estimating the future spatial configuration of ATE as well as for further development of models for various climates and latitudes. Furthermore, this study can easily be adapted to other satellite data and enable higher resolution results.

A future research direction would be improving the unmixing step and validating abundances using high-resolution images. Moreover, adaptation of this algorithm to be used with Sentinel-2 data would provide valuable information. Another research direction would be to test the algorithm at other mountains.

## REFERENCES

- Baddeley, A., Rubak, E., Turner, R., 2015. *Spatial Point Patterns: Methodology and Applications with R*. Chapman and Hall/CRC Press, 2015.
- Bader, M.Y., Ruijten, J.J.A., 2008. A topography-based model of forest cover at the alpine tree line in the tropical Andes. *J. Biogeogr.* 35, 711–723. <https://doi.org/10.1111/j.1365-2699.2007.01818.x>
- Barati, S., Rayegani, B., Saati, M., Sharifi, A., Nasri, M., 2011. Comparison the accuracies of different spectral indices for estimation of vegetation cover fraction in sparse vegetated areas. *Egypt. J. Remote Sens. Space Sci.* 14, 49–56. <https://doi.org/10.1016/j.ejrs.2011.06.001>
- Breiman, L., 2001. Random Forests. *Mach. Learn.* 45, 5–32. <https://doi.org/10.1023/A:1010933404324>
- Brenning, A., Bangs, D., Becker, M., 2018. *RSAGA: SAGA Geoprocessing and Terrain Analysis*.
- Butler, D.R., Malanson, G.P., Walsh, S.J., Fagre, D.B., 2007. Influences of Geomorphology and Geology on Alpine Treeline in the American West—More Important than Climatic Influences? *Phys. Geogr.* 28, 434–450. <https://doi.org/10.2747/0272-3646.28.5.434>
- Caccianiga, M., Andreis, C., Armiraglio, S., Leonelli, G., Pelfini, M., Sala, D., 2008. Climate continentality and treeline species distribution in the Alps. *Plant Biosyst. - Int. J. Deal. Asp. Plant Biol.* 142, 66–78. <https://doi.org/10.1080/11263500701872416>
- Cairns, D.M., Malanson, G.P., 1998. Environmental variables influencing the carbon balance at the alpine treeline: a modeling approach. *J. Veg. Sci.* 9, 679–692. <https://doi.org/10.2307/3237286>
- Cairns, D.M., Waldron, J.D., 2003. Sigmoid wave transitions at alpine treeline. *Geogr. Ann. Ser. Phys. Geogr.* 85, 115–126. <https://doi.org/10.1111/1468-0459.00193>
- Chen, B., Huang, B., Chen, L., Xu, B., 2017. Spatially and Temporally Weighted Regression: A Novel Method to Produce Continuous Cloud-Free Landsat Imagery. *IEEE Trans. Geosci. Remote Sens.* 55, 27–37. <https://doi.org/10.1109/TGRS.2016.2580576>

- Chen, Y., Lu, D., Luo, G., Huang, J., 2015. Detection of vegetation abundance change in the alpine tree line using multitemporal Landsat Thematic Mapper imagery. *Int. J. Remote Sens.* 36, 4683–4701. <https://doi.org/10.1080/01431161.2015.1088675>
- Chhetri, P.K., Thai, E., 2019. Remote sensing and geographic information systems techniques in studies on treeline ecotone dynamics. *J. For. Res.* 30, 1543–1553. <https://doi.org/10.1007/s11676-019-00897-x>
- Dalen, L., Hofgaard, A., 2005. Differential Regional Treeline Dynamics in the Scandes Mountains. *Arct. Antarct. Alp. Res.* 37, 284–296. [https://doi.org/10.1657/1523-0430\(2005\)037\[0284:DRTDIT\]2.0.CO;2](https://doi.org/10.1657/1523-0430(2005)037[0284:DRTDIT]2.0.CO;2)
- Dearborn, K.D., Danby, R.K., 2017. Aspect and slope influence plant community composition more than elevation across forest–tundra ecotones in subarctic Canada. *J. Veg. Sci.* 28, 595–604. <https://doi.org/10.1111/jvs.12521>
- Dinca, L., Nita, M.D., Hofgaard, A., Alados, C.L., Broll, G., Borz, S.A., Wertz, B., Monteiro, A.T., 2017. Forests dynamics in the montane–alpine boundary: a comparative study using satellite imagery and climate data. *Clim. Res.* 73, 97–110. <https://doi.org/10.3354/cr01452>
- Elliott, G.P., Cowell, C.M., 2015. Slope Aspect Mediates Fine-Scale Tree Establishment Patterns at Upper Treeline during Wet and Dry Periods of the 20th Century. *Arct. Antarct. Alp. Res.* 47, 681–692. <https://doi.org/10.1657/AAAR0014-025>
- Elliott, G.P., Kipfmüller, K.F., 2010. Multi-scale Influences of Slope Aspect and Spatial Pattern on Ecotonal Dynamics at Upper Treeline in the Southern Rocky Mountains, U.S.A. *Arct. Antarct. Alp. Res.* 42, 45–56. <https://doi.org/10.1657/1938-4246-42.1.45>
- Elliott, G.P., Petruccioli, C.A., 2018. Tree recruitment at the treeline across the Continental Divide in the Northern Rocky Mountains, USA: the role of spring snow and autumn climate. *Plant Ecol. Divers.* 11, 319–333. <https://doi.org/10.1080/17550874.2018.1487475>
- Farina, A., 2008. *Principles and Methods in Landscape Ecology: Towards a Science of the Landscape.* Springer Science & Business Media.
- Fisher, J.C., 2020. *inlmisc---Miscellaneous functions for the U.S. Geological Survey Idaho National Laboratory Project Office: U.S. Geological Survey software release, R package, Reston, Va.*
- Fisher, P., Arnot, C., Wadsworth, R., Wellens, J., 2006. Detecting change in vague interpretations of landscapes. *Ecol. Inform.* 1, 163–178. <https://doi.org/10.1016/j.ecoinf.2006.02.002>

- Fissore, V., Motta, R., Palik, B., Mondino, E.B., 2015. The role of spatial data and geomatic approaches in treeline mapping: a review of methods and limitations. *Eur. J. Remote Sens.* 48, 777–792. <https://doi.org/10.5721/EuJRS20154843>
- Fox, E.W., Hill, R.A., Leibowitz, S.G., Olsen, A.R., Thornbrugh, D.J., Weber, M.H., 2017. Assessing the accuracy and stability of variable selection methods for random forest modeling in ecology. *Environ. Monit. Assess.* 189, 316. <https://doi.org/10.1007/s10661-017-6025-0>
- Franc, V., Hlaváč, V., Navara, M., 2005. Sequential Coordinate-Wise Algorithm for the Non-negative Least Squares Problem, in: Gagalowicz, A., Philips, W. (Eds.), *Computer Analysis of Images and Patterns, Lecture Notes in Computer Science*. Springer, Berlin, Heidelberg, pp. 407–414. [https://doi.org/10.1007/11556121\\_50](https://doi.org/10.1007/11556121_50)
- Gehrig- Fasel, J., Guisan, A., Zimmermann, N.E., 2007. Tree line shifts in the Swiss Alps: Climate change or land abandonment? *J. Veg. Sci.* 18, 571–582. <https://doi.org/10.1111/j.1654-1103.2007.tb02571.x>
- Gorelic, N., Hancher, M., Dixon, M., Ilyushchenko, S., David, T., Moore, R., 2017. Google Earth Engine: Planetary-scale geospatial analysis for everyone. *Remote Sens. Environ.* <https://doi.org/10.1016/j.rse.2017.06.031>
- Grace, J., Berninger, F., Nagy, L., 2002. Impacts of Climate Change on the Tree Line. *Ann. Bot.* 90, 537–544. <https://doi.org/10.1093/aob/mcf222>
- Harsch, M.A., Hulme, P.E., McGlone, M.S., Duncan, R.P., 2009. Are treelines advancing? A global meta-analysis of treeline response to climate warming. *Ecol. Lett.* 12, 1040–1049. <https://doi.org/10.1111/j.1461-0248.2009.01355.x>
- Hijmans, R.J., 2020. raster package.
- Hill, R.A., Granica, K., Smith, G.M., Schardt, M., 2007. Representation of an alpine treeline ecotone in SPOT 5 HRG data. *Remote Sens. Environ., ForestSAT Special Issue 110*, 458–467. <https://doi.org/10.1016/j.rse.2006.11.031>
- Ho, T.K., 1995. Random decision forests, in: *Proceedings of 3rd International Conference on Document Analysis and Recognition*. Presented at the Proceedings of 3rd International Conference on Document Analysis and Recognition, pp. 278–282 vol.1. <https://doi.org/10.1109/ICDAR.1995.598994>
- Holtmeier, F.-K., 2009. *Mountain Timberlines: Ecology, Patchiness, and Dynamics*. Springer Science & Business Media.

- Hufkens, K., Ceulemans, R., Scheunders, P., 2008. Estimating the ecotone width in patchy ecotones using a sigmoid wave approach. *Ecol. Inform.* 3, 97–104. <https://doi.org/10.1016/j.ecoinf.2008.01.001>
- Ji, C.Y., 2008. Haze reduction from the visible bands of LANDSAT TM and ETM+ images over a shallow water reef environment. *Remote Sens. Environ., Remote Sensing Data Assimilation Special Issue* 112, 1773–1783. <https://doi.org/10.1016/j.rse.2007.09.006>
- Ju, J., Roy, D.P., 2008. The availability of cloud-free Landsat ETM+ data over the conterminous United States and globally. *Remote Sens. Environ.* 112, 1196–1211. <https://doi.org/10.1016/j.rse.2007.08.011>
- Karahalil, U., Kadioğullari, A.İ., Başkent, E.Z., Köse, S., 2009. The spatiotemporal forest cover changes in Köprülü Canyon National Park (1965 - 2008) in Turkey. *Afr. J. Biotechnol.* 8, 14.
- Kennedy, R.E., Andréfouët, S., Cohen, W.B., Gómez, C., Griffiths, P., Hais, M., Healey, S.P., Helmer, E.H., Hostert, P., Lyons, M.B., Meigs, G.W., Pflugmacher, D., Phinn, S.R., Powell, S.L., Scarth, P., Sen, S., Schroeder, T.A., Schneider, A., Sonnenschein, R., Vogelmann, J.E., Wulder, M.A., Zhu, Z., 2014. Bringing an ecological view of change to Landsat-based remote sensing. *Front. Ecol. Environ.* 12, 339–346. <https://doi.org/10.1890/130066>
- Kerr, J.T., Ostrovsky, M., 2003. From space to species: ecological applications for remote sensing. *Trends Ecol. Evol.* 18, 299–305. [https://doi.org/10.1016/S0169-5347\(03\)00071-5](https://doi.org/10.1016/S0169-5347(03)00071-5)
- Körner, C., 2012. *Alpine treelines : functional ecology of the global high elevation tree limits.* Springer, Basel.
- Körner, C., Hoch, G., 2006. A Test of Treeline Theory on a Montane Permafrost Island. *Arct. Antarct. Alp. Res.* 38, 113–119. [https://doi.org/10.1657/1523-0430\(2006\)038\[0113:ATOTTO\]2.0.CO;2](https://doi.org/10.1657/1523-0430(2006)038[0113:ATOTTO]2.0.CO;2)
- Kullman, L., 2005. Wind-Conditioned 20th Century Decline of Birch Treeline Vegetation in the Swedish Scandes. *Arctic* 58, 286–294.
- Kullman, L., 1979. Change and stability in the altitude of the birch tree-limit in the southern Swedish Scandes 1915-1975, *Acta phytogeographica Suecica* ; 65. Sv. växtgeografiska sällsk. ; Almqvist & Wiksell international (distr.), Uppsala : Stockholm.
- Landry, S., St-Laurent, M.-H., Nelson, P.R., Pelletier, G., Villard, M.-A., 2018. Canopy Cover Estimation from Landsat Images: Understorey Impact on Top-of-canopy Reflectance in a Northern Hardwood Forest. *Can. J. Remote Sens.* 44, 435–446. <https://doi.org/10.1080/07038992.2018.1533399>



- Leutner, B., Horning, N., Schwalb-Willmann, J., Hijmans, R.J., 2019. RStoolbox package.
- Liaw, A., Wiener, M., 2002. Classification and Regression by randomForest. *R News* 2, 18–22.
- Lin, C.-H., Lai, K.-H., Chen, Z.-B., Chen, J.-Y., 2014. Patch-Based Information Reconstruction of Cloud-Contaminated Multitemporal Images. *IEEE Trans. Geosci. Remote Sens.* 52, 163–174. <https://doi.org/10.1109/TGRS.2012.2237408>
- Maher, C.T., Millar, C.I., Affleck, D.L.R., Keane, R.E., Sala, A., Tobalske, C., Larson, A.J., Nelson, C.R., 2021. Alpine treeline ecotones are potential refugia for a montane pine species threatened by bark beetle outbreaks. *Ecol. Appl.* 31, e2274. <https://doi.org/10.1002/eap.2274>
- Malanson, G.P., Butler, D.R., 1994. Tree-Tundra Competitive Hierarchies, Soil Fertility Gradients, and Treeline Elevation in Glacier National Park, Montana. *Phys. Geogr.* 15, 166–180. <https://doi.org/10.1080/02723646.1994.10642511>
- Malanson, G.P., Butler, D.R., Fagre, D.B., Walsh, S.J., Tomback, D.F., Daniels, L.D., Resler, L.M., Smith, W.K., Weiss, D.J., Peterson, D.L., Bunn, A.G., Hiemstra, C.A., Liptzin, D., Bourgeron, P.S., Shen, Z., Millar, C.I., 2013. Alpine Treeline of Western North America: Linking Organism-To-Landscape Dynamics. *Phys. Geogr.* 28, 378–396. <https://doi.org/10.2747/0272-3646.28.5.378>
- Man, C.D., Nguyen, T.T., Bui, H.Q., Lasko, K., Nguyen, T.N.T., 2018. Improvement of land-cover classification over frequently cloud-covered areas using Landsat 8 time-series composites and an ensemble of supervised classifiers. *Int. J. Remote Sens.* 39, 1243–1255. <https://doi.org/10.1080/01431161.2017.1399477>
- Mancino, G., Nolè, A., Ripullone, F., Ferrara, A., 2014. Landsat TM imagery and NDVI differencing to detect vegetation change: assessing natural forest expansion in Basilicata, southern Italy. *IForest - Biogeosciences For.* 7, 75. <https://doi.org/10.3832/ifor0909-007>
- Masek, J.G., 2001. Stability of boreal forest stands during recent climate change: evidence from Landsat satellite imagery. *J. Biogeogr.* 28, 967–976. <https://doi.org/10.1046/j.1365-2699.2001.00612.x>
- McCaffrey, D.R., Hopkinson, C., 2020. Modeling Watershed-Scale Historic Change in the Alpine Treeline Ecotone Using Random Forest. *Can. J. Remote Sens.* 46, 715–732. <https://doi.org/10.1080/07038992.2020.1865792>

- Müller, M., Oelmann, Y., Schickhoff, U., Böhner, J., Scholten, T., 2017. Himalayan treeline soil and foliar C:N:P stoichiometry indicate nutrient shortage with elevation. *Geoderma* 291, 21–32. <https://doi.org/10.1016/j.geoderma.2016.12.015>
- NASA, 2021. Landsat 4-5 Thematic Mapper (TM) Level-1 Data Products [WWW Document]. *Landsat Sci.* URL <https://landsat.gsfc.nasa.gov/landsat-4-5> (accessed 9.4.21).
- NASA, 2019. ASTER GDEM.
- Potter, C., 2016. Vegetation Cover Change in Glacier National Park Detected using 25 Years of Landsat Satellite Image Analysis. *J. Biodivers. Manag. For.* 05. <https://doi.org/10.4172/2327-4417.1000152>
- Potter, C., Dolanc, C., 2016. Thirty Years of Change in Subalpine Forest Cover from Landsat Image Analysis in the Sierra Nevada Mountains of California. *For. Sci.* 62, 623–632. <https://doi.org/10.5849/forsci.15-145>
- R Core Team, 2020. R: A language and environment for statistical computing. R Foundation for Statistical Computing, Vienna, Austria.
- Resler, L.M., 2006. Geomorphic Controls of Spatial Pattern and Process at Alpine Treeline. *Prof. Geogr.* 58, 124–138. <https://doi.org/10.1111/j.1467-9272.2006.00520.x>
- Resler, L.M., Shao, Y., Tomback, D.F., Malanson, G.P., 2014. Predicting Functional Role and Occurrence of Whitebark Pine (*Pinus albicaulis*) at Alpine Treelines: Model Accuracy and Variable Importance. *Ann. Assoc. Am. Geogr.* 104, 703–722. <https://doi.org/10.1080/00045608.2014.910072>
- Rogers, A.S., Kearney, M.S., 2004. Reducing signature variability in unmixing coastal marsh Thematic Mapper scenes using spectral indices. *Int. J. Remote Sens.* 25, 2317–2335. <https://doi.org/10.1080/01431160310001618103>
- Senf, C., Laštovička, J., Okujeni, A., Heurich, M., van der Linden, S., 2020. A generalized regression-based unmixing model for mapping forest cover fractions throughout three decades of Landsat data. *Remote Sens. Environ.* 240, 111691. <https://doi.org/10.1016/j.rse.2020.111691>
- Shahtahmassebi, A., Ning, Y., Ke, W., Moore, N., Zhangquan, S., 2013. Review of Shadow Detection and De-shadowing Methods in Remote Sensing. *Chin. Geogr. Sci.* 23, 18.
- Sigdel, S.R., Wang, Y., Camarero, J.J., Zhu, H., Liang, E., Peñuelas, J., 2018. Moisture-mediated responsiveness of treeline shifts to global warming in the Himalayas. *Glob. Change Biol.* 24, 5549–5559. <https://doi.org/10.1111/gcb.14428>

- Strimas-Mackey, M., 2021. smoothr: Smooth and Tidy Spatial Features. R package version 0.2.2.
- Walsh, S.J., Butler, D.R., Allen, T.R., Malanson, G.P., 1994. Influence of snow patterns and snow avalanches on the alpine treeline ecotone. *J. Veg. Sci.* 5, 657–672. <https://doi.org/10.2307/3235881>
- Weiss, D.J., Malanson, G.P., Walsh, S.J., 2015. Multiscale Relationships Between Alpine Treeline Elevation and Hypothesized Environmental Controls in the Western United States. *Ann. Assoc. Am. Geogr.* 105, 437–453. <https://doi.org/10.1080/00045608.2015.1015096>
- Weiss, D.J., Walsh, S.J., 2009. Remote Sensing of Mountain Environments. *Geogr. Compass* 3, 1–21. <https://doi.org/10.1111/j.1749-8198.2008.00200.x>
- Wielgolaski, F.E., Hofgaard, A., Holtmeier, F.K., 2017. Sensitivity to environmental change of the treeline ecotone and its associated biodiversity in European mountains. *Clim. Res.* 73, 151–166. <https://doi.org/10.3354/cr01474>
- Zhang, Y., Xu, M., Adams, J., Wang, X., 2009. Can Landsat imagery detect tree line dynamics? *Int. J. Remote Sens.* 30, 1327–1340. <https://doi.org/10.1080/01431160802509009>
- Zong, S., Wu, Z., Xu, J., Li, M., Gao, X., He, H., Du, H., Wang, L., 2014. Current and Potential Tree Locations in Tree Line Ecotone of Changbai Mountains, Northeast China: The Controlling Effects of Topography. *PLOS ONE* 9, e106114. <https://doi.org/10.1371/journal.pone.0106114>